

SMALL HYPERBOLIC POLYHEDRA

SHAWN RAFALSKI

Department of Mathematics and Computer Science
Fairfield University
Fairfield, CT 06824, USA
srafalski@fairfield.edu

ABSTRACT. We classify the 3-dimensional hyperbolic polyhedral orbifolds that contain no embedded essential 2-suborbifolds, up to decomposition along embedded hyperbolic triangle orbifolds (turnovers). We give a necessary condition for a 3-dimensional hyperbolic polyhedral orbifold to contain an immersed (singular) hyperbolic turnover, we classify the triangle subgroups of the fundamental groups of orientable 3-dimensional hyperbolic tetrahedral orbifolds in the case when all of the vertices of the tetrahedra are non-finite, and we provide a conjectural classification of all the triangle subgroups of the fundamental groups of orientable 3-dimensional hyperbolic polyhedral orbifolds. Finally, we show that any triangle subgroup of a (non-orientable) 3-dimensional hyperbolic reflection group arises from a triangle reflection subgroup.

1. INTRODUCTION

Let P be a finite volume 3-dimensional hyperbolic Coxeter polyhedron. That is, P is the finite volume intersection of a finite collection of half-spaces in hyperbolic 3-space \mathbb{H}^3 in which the bounding planes of each pair of intersecting half-spaces meet at an angle of the form π/n , where $n \geq 2$ is an integer (the geodesic of intersection is called an *edge* of P , and the angle of intersection is called the *dihedral angle* of P along this edge). Then the group of isometries of \mathbb{H}^3 generated by the reflections in the faces of P is a discrete group that acts on \mathbb{H}^3 with fundamental domain P . Let Γ be the subgroup of index two in this reflection group generated by all the rotations of the form rs , where r and s are the reflections through two intersecting planes that support P . We denote by \mathcal{O}_P the quotient space \mathbb{H}^3/Γ . Then \mathcal{O}_P is an orientable hyperbolic 3-orbifold called a *hyperbolic polyhedral orbifold*. The group Γ is sometimes denoted by $\pi_1(\mathcal{O}_P)$ and called the *fundamental group of \mathcal{O}_P* . We call P a *hyperbolic reflection polyhedron*.

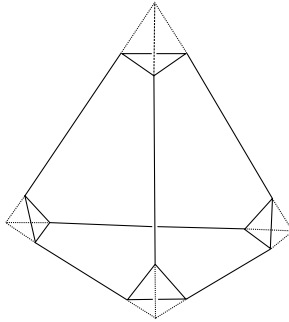
A *small* hyperbolic reflection polyhedron corresponds to a hyperbolic 3-dimensional polyhedral orbifold that contains no embedded essential 2-suborbifolds, up to decomposition along embedded triangular 2-suborbifolds (Definition 2.1). We classify these polyhedra (see Figure 1):

Theorem 1.1. *A 3-dimensional hyperbolic reflection polyhedron is small if and only if it is a generalized tetrahedron.*

Date: January 2011.

Mathematics Subject Classification (2010): 52B10, 57M50, 57R18.

Key words and phrases. Hyperbolic polyhedra, 3-dimensional Coxeter polyhedra, triangle groups, hyperbolic orbifold, polyhedral orbifold, small orbifold, essential suborbifold, hyperbolic turnover.

FIGURE 1. The small Coxeter polyhedra in \mathbb{H}^3

We also determine those hyperbolic polyhedral orbifolds that contain an immersed (singular) hyperbolic triangular 2-suborbifold. This result is a generalization of the partial classification of triangle groups inside of arithmetic hyperbolic tetrahedral reflection groups given by Maclachlan [8]. In Section 4, we will provide a conjectural list of all the possibilities for immersed turnovers in all polyhedral orbifolds:

Theorem 1.2. *If a hyperbolic polyhedral 3-orbifold contains a singular hyperbolic turnover that does not cover an embedded hyperbolic turnover, then at least one component of its Dunbar decomposition is a generalized tetrahedron, and the immersed turnover is contained in a unique such component. Furthermore, if T is a generalized tetrahedron with all non-finite vertices and whose associated polyhedral 3-orbifold contains an immersed turnover, then, up to symmetry, T is of the form $T[2, m, q; 2, p, 3]$ (in the notation described in Section 4) with $m \geq 6$, $q \geq 3$ and $p \geq 6$, and the immersed turnover has singular points of orders m , q and p .*

We also determine the triangle subgroups of 3-dimensional hyperbolic reflection groups as arising from triangle reflection subgroups:

Theorem 1.3. *Any (orientable) hyperbolic triangle subgroup of a (non-orientable) 3-dimensional hyperbolic reflection group G arises as a subgroup of index two of a (non-orientable) hyperbolic triangle reflection subgroup of G .*

Essential surfaces play an integral role in low-dimensional topology and geometry. One of the most important instances of this fact is the proof of Thurston's Hyperbolization Theorem for Haken 3-manifolds [16], [10]. In brief, Thurston's Theorem is proved by decomposing a given 3-manifold M (which is called *Haken* if it contains an essential surface) along such surfaces as part of a finite-step process that ends in topological solid balls, from which the hyperbolic structure on M (whose existence is claimed by the theorem) is then, in a sense, reverse-engineered.

One difficulty that arises in attempting to extend the utility of essential surfaces to the orbifold setting is the possible presence of triangular hyperbolic 2-dimensional suborbifolds called *hyperbolic turnovers*. For example, whereas an irreducible 3-manifold with non-empty and non-spherical boundary always contains an essential surface, this is not always the case in the orbifold setting, with hyperbolic turnovers

presenting the principal barrier. Thurston’s original definition of a Haken 3-orbifold was given for non-orientable 3-orbifolds with underlying space the 3-ball and with singular locus equal to the boundary of the ball [15, Section 13.5, p. 324]. (The singular locus, in this instance, was meant to correspond to the boundary of a polyhedron.) Subsequent formulations of the definition of Haken (i.e., “sufficiently large” in [6, Glossary] or “Haken” in [4, Section 4.2, Remark]) were given for the orientable case and take into account the difficulties that arise from hyperbolic turnovers. Theorem 1.1, which is proved using the same observations that Thurston used to determine 3-orbifolds with the combinatorial type of a simplex as the original “non-Haken” polyhedral orbifolds, echoes Thurston’s original result [15, Proposition 13.5.2], with respect to this evolution of the language.

Acknowledgments. The author thanks Ian Agol for helpful conversations. Very special thanks to the referee for invaluable feedback.

2. DEFINITIONS

There are several excellent references for orbifolds [4], [5]. All of the 3-orbifolds considered in this paper are either orientable hyperbolic polyhedral 3-orbifolds or the result of cutting an orientable hyperbolic polyhedral 3-orbifold along a finite set of totally geodesic hyperbolic turnovers or totally geodesic hyperbolic triangles with mirrored sides. A hyperbolic polyhedral 3-orbifold \mathcal{O}_P is geometrically just two copies of its associated hyperbolic polyhedron P with the corresponding sides of the two copies identified. Thus, \mathcal{O}_P is a complete metric space of constant curvature -1 except along a 1-dimensional singular subset which is locally cone-like. If P is compact, then \mathcal{O}_P is topologically a 3-sphere together with a trivalent planar graph (corresponding to the 1-skeleton of P) with each edge marked by a positive integer to represent the submultiple of π of the dihedral angle at the corresponding edge of P . If P is noncompact with finite volume, then its ideal vertices correspond to trivalent or quadrivalent vertices in the planar graph (again, corresponding to the 1-skeleton of P) and the sum of the reciprocals of the incident edge marks at each such vertex is equal to one or two, according to whether the vertex is trivalent or quadrivalent. In the noncompact case, \mathcal{O}_P is topologically the result of taking a 3-sphere with this marked graph and removing a (closed) 3-ball neighborhood from each ideal vertex. The statements about the combinatorics of hyperbolic polyhedra in this paragraph are consequences of Andreev’s Theorem [2], [3], [13], [15, Section 13.6], [7].

A (closed) orientable 2-orbifold is topologically a closed orientable surface with some finite set of its points marked by positive integers (greater than one). Every such 2-orbifold can be realized as a complete metric space of constant curvature with cone-like singularities at the marked points, and where the sign of the curvature depends only on the topology of the underlying surface together with the markings. A 2-orbifold is called *spherical*, *Euclidean* or *hyperbolic* according to the sign of its constant curvature realization. A *turnover* is a 2-orbifold that is topologically a 2-sphere with three marked points, and a *hyperbolic turnover* is a turnover for which

the reciprocal sum of the integer markings is less than one. Although we will seldom deal with non-orientable objects, we define a *hyperbolic triangle with mirrored sides* as a topological closed disk whose boundary is marked with three distinct points, each point labeled by an integer greater than one and such that the sum of the reciprocals of these integers is less than one, and with the connecting intervals in the boundary between these points marked as “mirrors.” Hyperbolic triangles with mirrored sides are non-orientable 2-orbifolds that are doubly covered by hyperbolic turnovers: they are the quotients of hyperbolic turnovers by an involution that fixes an embedded topological circle that passes through the marked points of the turnover. Every embedded hyperbolic turnover in a hyperbolic 3-orbifold can either be made totally geodesic by an isotopy in the 3-orbifold (in which case the preimage in \mathbb{H}^3 under the covering map of this totally geodesic 2-suborbifold is a collection of disjoint planes, each tiled by a hyperbolic triangle that is determined by the markings of the singular points (e.g., [9, Chapter IX.C], [1, Theorem 2.1])) or else can be moved by an isotopy to be the boundary of a regular neighborhood of a totally geodesic hyperbolic triangle with mirrored sides.

An embedded orientable 2-suborbifold of \mathcal{O}_P is topologically a surface that meets the marked graph transversely. We note that any simple closed curve $C \subset \partial P$ that meets the 1-skeleton transversely determines such a 2-suborbifold by adjoining to C the two topological disks that it bounds, one to either side of $\partial P \subset \mathcal{O}_P$. A closed path on ∂P that is isotopic to a simple circuit in the dual graph to the 1-skeleton of P is called a *k-circuit*, where k is the number of edges the path crosses. An embedded hyperbolic triangle with mirrored sides occurs as a suborbifold of \mathcal{O}_P whenever P has a triangular face all of whose edges are labeled two (in this case, the triangle with mirrored sides is topologically just the disc bounded by these three edges in the marked graph).

The terminology of this paragraph is introduced in terms of general orbifolds. A compact *n-orbifold* \mathcal{O} with boundary is a metrizable topological space which is locally diffeomorphic either to the quotient of \mathbb{R}^n by a finite group action or to the quotient of $\mathbb{R}^{n-1} \times [0, \infty)$ by a finite group action, with points of the latter type making up the *boundary* $\partial\mathcal{O}$ of \mathcal{O} (itself an $(n - 1)$ -orbifold). We use the term *orbifold ball* (respectively, *orbifold disk*) to refer to the quotient of a compact 3-ball (respectively, 2-disk) by a finite group action. We say a compact 3-orbifold \mathcal{O} is *irreducible* if every embedded spherical 2-suborbifold bounds an orbifold ball in \mathcal{O} . A 2-suborbifold $F \subset \mathcal{O}$ is called *compressible* if either F is spherical and bounds an orbifold ball or if there is a simple closed curve in F that does not bound an orbifold disk in F but that bounds an orbifold disk in \mathcal{O} , and *incompressible* otherwise. There is a relative notion of ∂ -incompressibility (whose exact definition we do not require). We call F *essential* if it is incompressible, ∂ -incompressible and not parallel to a boundary component of \mathcal{O} . We call a compact irreducible 3-orbifold *Haken* if it is either an orbifold ball, or a turnover crossed with an interval, or if it contains an essential 2-suborbifold but contains no essential turnover. A compact irreducible

3-orbifold is called *small* if it contains no essential 2-suborbifolds and has (possibly empty) boundary consisting only of turnovers. (We note that a compact, orientable and irreducible orbifold is both Haken and small if and only if it is either a cone on a spherical turnover or a product of a turnover with an interval.) These definitions extend to any arbitrary 3-orbifold that is diffeomorphic to the interior of a compact 3-orbifold with boundary.

We observe that Euclidean and hyperbolic turnovers are always incompressible because a simple closed curve on these objects always bounds an orbifold disk. As a consequence, in an irreducible 3-orbifold, any incompressible 2-orbifold (in fact, even any singular hyperbolic turnover) can be made disjoint from an embedded hyperbolic turnover.

Remark 1. It is a consequence of a theorem proved by Dunbar that a hyperbolic polyhedral 3-orbifold can be decomposed (uniquely, up to isotopy) along a system of essential, pairwise non-parallel hyperbolic turnovers into pieces that contain no essential (embedded) turnovers, and, moreover, that each component of the decomposition is either a Haken or a small 3-orbifold ([6], [4, Theorem 4.8]). An embedded hyperbolic turnover in a hyperbolic polyhedral 3-orbifold \mathcal{O}_P will correspond to a simple closed curve in ∂P that crosses exactly three edges whose dihedral angles sum to less than π . If such a curve is parallel in ∂P to a triangular face of P all of whose edges are labeled two, then the hyperbolic turnover corresponding to this curve is isotopic to the boundary of a regular neighborhood of a hyperbolic triangle with mirrored sides (the latter arising from the triangular face of P) in \mathcal{O}_P . In this case, one component of the Dunbar decomposition will consist of the regular neighborhood of this triangle with mirrored sides (in fact, this is a small 3-orbifold). The complement of this component in \mathcal{O}_P is (orbifold) diffeomorphic to the complement of the triangle with mirrored sides in \mathcal{O}_P (because the hyperbolic turnover collapses onto the mirrored triangle as the radius of the regular neighborhood goes to zero), and so, for convenience, we discard the component of the Dunbar decomposition corresponding to this regular neighborhood.

With the above convention in mind, we have the following:

Definition 2.1. *A hyperbolic reflection polyhedron P is small if the Dunbar decomposition of \mathcal{O}_P (with the convention of the preceding paragraph) consists of a single connected small component.*

In the projective model of \mathbb{H}^3 , consider a linearly independent set of four points, any or all of which may lie on the boundary of or outside of the projective ball. If the line segment between each pair of these points intersects the interior of the projective ball, then the points determine a *generalized tetrahedron*. This polyhedron is obtained by taking the (possibly infinite volume) polyhedron in \mathbb{H}^3 spanned by the points and truncating its infinite volume ends by the dual hyperplanes to the super-ideal vertices. The resulting polyhedron has finite volume and all of its vertices are either finite or ideal. The faces arising from truncated super-ideal vertices—which are

called, along with the finite and ideal vertices, *generalized vertices*—are triangular, and the dihedral angle at each edge of these faces is $\pi/2$. In particular, if a generalized tetrahedron P is a Coxeter polyhedron, then any generalized vertex arising from a truncated face is a hyperbolic triangle that tiles (under the tiling associated to P) a geodesic plane in \mathbb{H}^3 (and thus gives rise to an embedded hyperbolic triangle with mirrored sides in \mathcal{O}_P).

3. PROOF OF THEOREM 1.1

Proof of 1.1. Let P be a 3-dimensional hyperbolic Coxeter polyhedron, and let \mathcal{O}_P be its hyperbolic polyhedral 3-orbifold. First assume that P is a generalized tetrahedron. Then \mathcal{O}_P is topologically the 3-sphere with a marked planar graph as in Figure 2. Each dot in the figure represents a generalized vertex, and so is either a

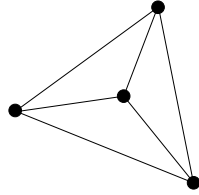


FIGURE 2. The graph associated to a generalized tetrahedron

finite vertex, a triangle with mirrored sides or a Euclidean turnover cusp (the latter if the vertex is ideal). Any dot that represents a triangle corresponds to a non-separating hyperbolic turnover of the Dunbar decomposition of \mathcal{O}_P . Moreover, since any two hyperbolic turnovers can be made disjoint by an isotopy, any other turnovers in the Dunbar decomposition occur as topological 2-spheres that intersect the graph from the figure in exactly three distinct edges. But the only possibility for such a 2-sphere is one that surrounds a dot, and that therefore is parallel to a generalized vertex of P . So the Dunbar decomposition of \mathcal{O}_P (under the convention of Definition 2.1) has a single component.

To see that this component is small, we consider the graph of Figure 2 as the 1-skeleton of a tetrahedron in the 3-sphere. Using standard topology arguments, it can be shown that an incompressible 2-suborbifold intersects the interior of this tetrahedron in triangles and quadrilaterals. But a triangular intersection implies that the incompressible 2-suborbifold is isotopic to the hyperbolic turnover associated to a generalized vertex, and a quadrilateral intersection produces a compression. So P is small if it is a generalized tetrahedron.

Now assume that P is small. The rest of the proof of Theorem 1.1 depends on the following simple observation [15, Proposition 13.5.2]:

Remark 2. Suppose that $C \subset \partial P$ is a simple closed curve that is transverse to, forms no bigons with, does not surround a single vertex of, and that crosses at least two distinct edges of the 1-skeleton of P . Then C determines an incompressible 2-suborbifold of \mathcal{O}_P if and only if (1) it intersects any face in a connected set or

not at all and (2) it intersects the common edge of two adjacent faces whenever its intersection with both faces is nonempty.

We begin with the following fact about triangular faces of P :

Lemma 3.1. *If T is a triangular face of P , then T corresponds to a hyperbolic turnover in \mathcal{O}_P or P is a generalized tetrahedron.*

Proof of 3.1. Suppose that T is as in Figure 3a (in this and all subsequent figures in this section, we depict P by a planar projection). If $1/p + 1/q + 1/r \geq 1$, then the three edges incident to the vertices of T must intersect (or meet at a Euclidean turnover) [13, Lemmata 3.2 and 3.3], in which case P is a generalized tetrahedron (possibly with an ideal vertex). Otherwise, we have $1/p + 1/q + 1/r < 1$. Then the 3-circuit around this face determines a hyperbolic turnover in \mathcal{O}_P whose associated triangle in P must be boundary-parallel (in P) because P is small. The two possibilities are shown in Figures 3b (in which the hyperbolic turnover collapses to the outermost face) and 3c (in which the hyperbolic turnover collapses to T). 3.1

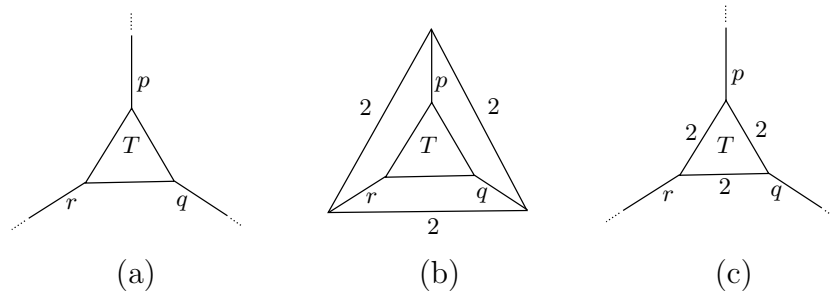
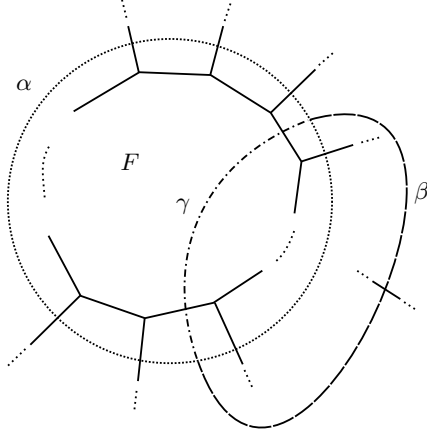


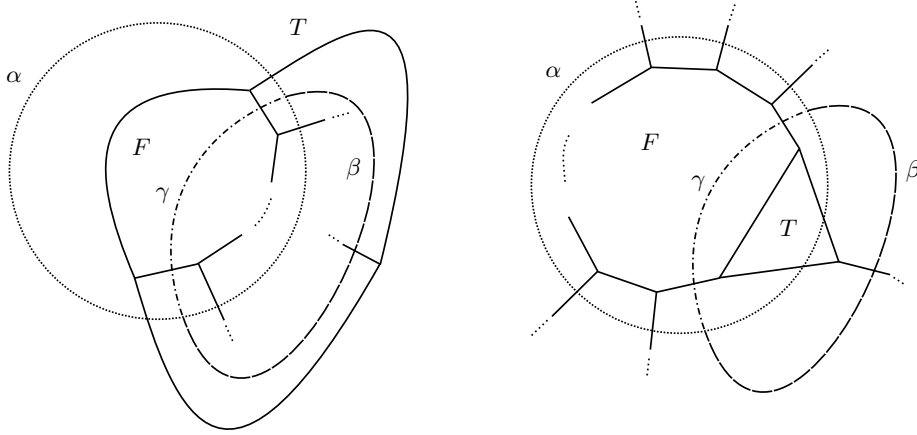
FIGURE 3. Triangular faces

Throughout the rest of the proof, we will use the observation from the above lemma, i.e., that any 3-circuit in a small hyperbolic polyhedron surrounds a generalized vertex. In the case when the 3-circuit determines a hyperbolic turnover, this follows by the fact that a hyperbolic turnover in a hyperbolic 3-orbifold always corresponds to a totally geodesic 2-suborbifold (according to the second paragraph in Section 2; compare also with the incompressibility observation in the paragraph preceding Remark 1): Because the polyhedron P is small, this totally geodesic 2-suborbifold of \mathcal{O}_P cannot be an embedded hyperbolic turnover (because \mathcal{O}_P has no boundary, and so such a turnover would have to be essential), and therefore must be a triangle with mirrored sides that corresponds to a triangular face of P .

Consider an n -sided face F of P , as in Figure 4. Assume that $n \geq 4$. The n -circuit α around F determines a 2-orbifold that must be compressible, with a compressing orbifold disk whose intersection with ∂P appears as the dashed arc β in the figure. Since $n \geq 4$, it must be that each side of the 3-circuit $\beta \cup \gamma$ contains at least two edges radiating outward from F (that is, edges meeting F only in vertices). Since \mathcal{O}_P

FIGURE 4. A face of P and a compression

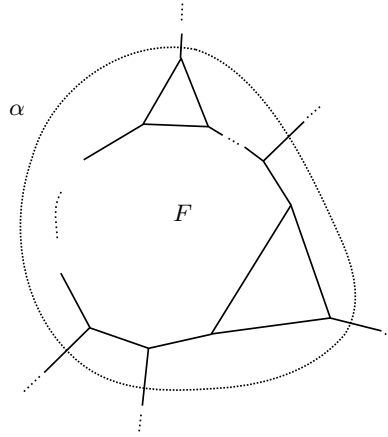
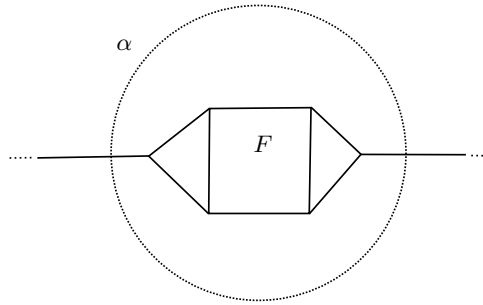
is small, $\beta \cup \gamma$ bounds a triangle $T \subset \partial P$. Figure 5 illustrates the two possibilities, depending on the side of $\beta \cup \gamma$ to which T lies. Of course, these differ only by the choice of projection of P into the plane.

FIGURE 5. Two projections of a face of P with adjacent triangle

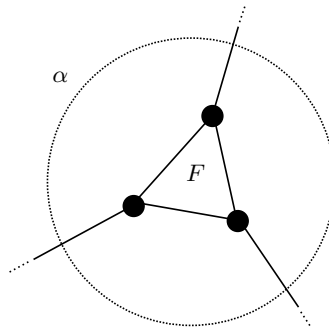
We now consider all such compressions of this 2-orbifold, and all of the resulting adjacent triangles to F . Let α denote the k -circuit that encloses F and these triangles, as in Figure 6.

If $k = 2$, then F must be a quadrilateral with two triangles adjacent to it on opposite sides, in which case P is a triangular prism with one face that corresponds to a hyperbolic turnover in \mathcal{O}_P as in Lemma 3.1, i.e., P is a generalized tetrahedron. See Figure 7.

If $k = 3$, then α surrounds a generalized vertex to the outside. In this case, the face F must be as in Figure 8, where each dot represents either a finite vertex, an

FIGURE 6. A face of P with all of its adjacent triangles, and a k -circuitFIGURE 7. A face of P with all of its adjacent triangles, and a 2-circuit

ideal vertex or a hyperbolic triangle. Filling in the generalized vertex to the outside of α , we have that P is a generalized tetrahedron.

FIGURE 8. A face of P with all of its adjacent triangles, and a 3-circuit

If $k > 3$, then the 2-orbifold determined by α has a compression. But any such compression would add an adjacent triangular face to F , and we have assumed that α encloses all such triangles. So $k \leq 3$. This completes the proof. 1.1

4. TURNOVERS IN HYPERBOLIC POLYHEDRA

In this final section, we prove Theorems 1.2 and 1.3, and provide a classification of the immersed hyperbolic turnovers in those tetrahedral orbifolds that arise from tetrahedra with no finite vertices. Although Theorem 1.3 does not follow from Theorem 1.2, we will provide the proof of the former in the midst of the proof of the latter, as it contains an observation that is necessary for both proofs.

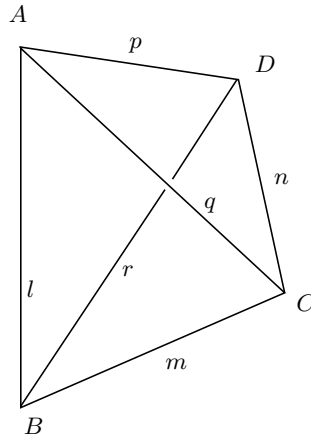
The author showed that if a hyperbolic 3-orbifold contains a singular hyperbolic turnover, then that turnover must be contained in a low-volume small 3-suborbifold [11]. In particular, we have the following

Theorem 4.1. *(Theorem 1.1 and Corollary 1.3 in [11]) Let Q be a compact, irreducible, orientable, atoroidal 3-orbifold. Then any immersion $f: \mathcal{T} \rightarrow Q$ of a hyperbolic turnover into Q is homotopic into a unique component of the Dunbar decomposition of Q , up to covers of parallel boundary components of the decomposition. Moreover, if f is a singular immersion that does not cover an embedded turnover or triangle with mirrored sides, then the component containing $f(\mathcal{T})$ is unique, and it is a small 3-orbifold.*

Proof of 1.2. If \mathcal{O}_P is a hyperbolic polyhedral 3-orbifold, then it is homeomorphic to the interior of an orbifold that satisfies the hypotheses of Theorem 4.1. If \mathcal{O}_P contains a singular turnover, then this turnover is contained in a small component of the Dunbar decomposition of \mathcal{O}_P , and Theorem 1.1 classifies these small orbifolds as generalized tetrahedral orbifolds.

It remains to provide a classification of the generalized tetrahedra whose associated 3-orbifolds contain immersed turnovers. We will do so for generalized tetrahedra all of whose vertices are non-finite. *See the summary at the end of the paper for the results of the classification.* The techniques we use to provide this classification can be used to classify the immersed turnovers in all tetrahedral orbifolds, thereby extending and completing the classification begun by Maclachlan in the case of compact (non-generalized) tetrahedral orbifolds [8], however, the case-by-case analysis required to complete this classification in general is somewhat excessive.

We let $T[l, m, q; n, p, r]$ denote the hyperbolic generalized tetrahedron $ABCD$ with dihedral angles $\pi/l, \pi/m, \pi/q, \pi/n, \pi/p$ and π/r , as in Figure 9, with the convention that a vertex of T is truncated (respectively, ideal) if the dihedral angles of its three coincident edges sum to less than (respectively, equal to) π . The conditions on l, m, q, n, p and r guaranteeing the existence of $T[l, m, q; n, p, r]$ are known [18]. In particular, there are nine compact (non-truncated) tetrahedra (e.g. [12, Chapter 7]), all of whose associated orbifolds contain singular turnovers. We note that, of the nine compact (non-truncated) tetrahedra, eight yield arithmetic hyperbolic 3-orbifolds. As we noted above, Maclachlan classified almost all of the immersed turnovers in these arithmetic tetrahedral orbifolds using arithmetic methods. Our geometric technique can be considered as an alternative means to prove (and extend) those results, without appeal to arithmeticity.

FIGURE 9. $T[l, m, q; n, p, r]$

Denote by \mathcal{O}_T the 3-orbifold determined by $T[l, m, q; n, p, r]$. Recall from Section 2 that any hyperbolic turnover in a hyperbolic 3-orbifold that does not collapse onto a hyperbolic triangle with mirrored sides may be assumed to be totally geodesic. It also follows from the incompressibility of hyperbolic turnovers in irreducible orbifolds that an immersed turnover must be disjoint from any embedded turnover [11, Lemma 5.3]. Consequently, if \mathcal{T} is a hyperbolic turnover, then an immersion $f: \mathcal{T} \rightarrow \mathcal{O}_T$ lifts to the universal cover \mathbb{H}^3 as a collection of geodesic planes with some intersections—two or more of these planes will intersect whenever there is a covering transformation (i.e., an element of the fundamental group $\pi_1(\mathcal{O}_T)$ of \mathcal{O}_T , which is just the group of isometries of \mathbb{H}^3 that yields the quotient \mathcal{O}_T) that does not move one plane completely disjoint from some of the others, and this must occur if there is a singular immersion of a turnover in \mathcal{O}_T —and, additionally, the collection of planes determined by an immersed turnover must be disjoint from the collection of planes determined by any turnover corresponding to a generalized vertex of T .

After these preliminaries, we now will prove Theorem 1.3.

Proof of 1.3. Let $P \subset \mathbb{H}^3$ be a polyhedron that generates the non-orientable 3-dimensional hyperbolic polyhedral reflection group G , and let $S \subset G$ be an orientable triangle subgroup. Then S is generated by two elliptic elements in G and stabilizes a plane $\Pi_S \subset \mathbb{H}^3$. In particular, Π_S meets the axis of every element of S at a right angle, and the intersections of Π_S with these axes comprise the vertex set of a tiling of Π_S by hyperbolic triangles. Every such vertex will have k lines passing through it (where k is the order of the elliptic element stabilizing the vertex) that are the perpendicular intersections with Π_S of G -translates of a face of P . This set of lines and their intersections generates a tiling of Π_S by hyperbolic triangles that corresponds to a hyperbolic triangle with mirrored sides in the non-orientable hyperbolic orbifold \mathbb{H}^3/G , and this 2-orbifold is covered by the hyperbolic turnover corresponding to S . Therefore, S is contained in the triangle reflection subgroup of G that corresponds

to this non-orientable triangle 2-orbifold.

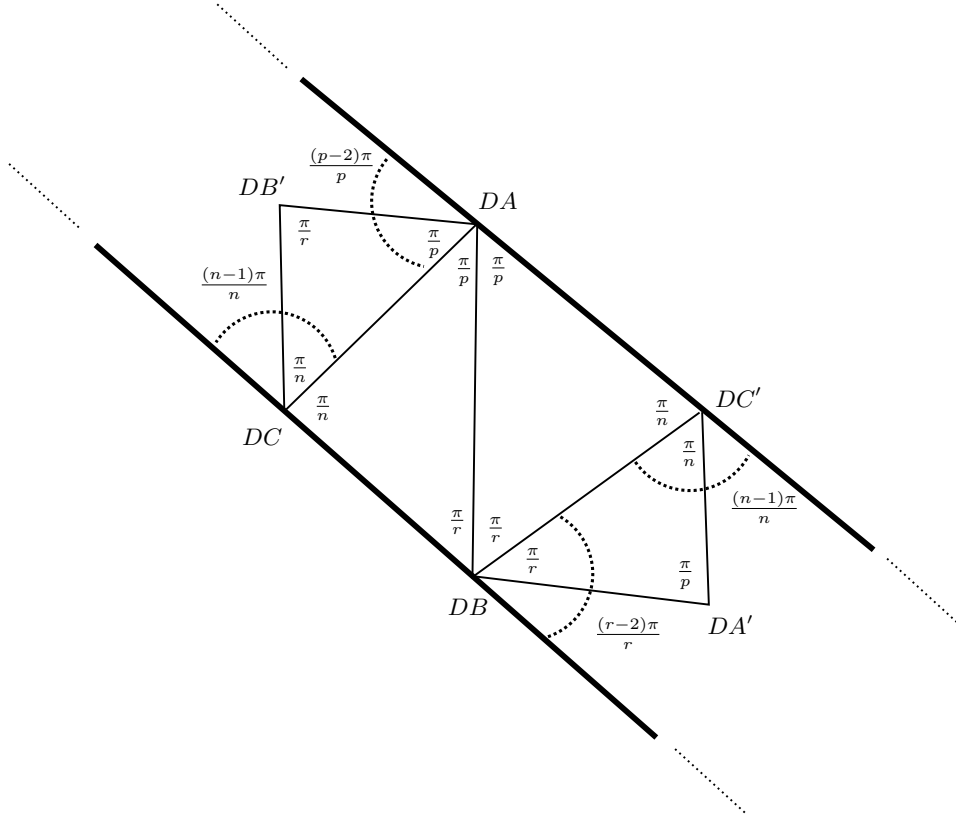
1.3

We take a moment to emphasize the observation from the above proof: Any maximal (orientable) triangle subgroup of 3-dimensional hyperbolic polyhedral reflection group has as a fundamental domain a triangle whose edges are contained in the faces of the corresponding polyhedral tiling of \mathbb{H}^3 (the edges may intersect multiple faces of the polyhedral tiling). This fact is used in the next paragraph.

Here is the strategy for classifying the immersed turnovers of \mathcal{O}_T (the proof is somewhat lengthy, but this paragraph contains the core idea): Let \mathcal{T} be a hyperbolic turnover. Up to conjugacy, there is a unique discrete orientation-preserving group of isometries of the hyperbolic plane \mathbb{H}^2 corresponding to the tiling of \mathbb{H}^2 by copies of the triangle that determines \mathcal{T} (the fundamental group $\pi_1(\mathcal{T})$ of \mathcal{T}). If $f: \mathcal{T} \rightarrow \mathcal{O}_T$ is an immersion, then f may be assumed to have totally geodesic image. Consider a plane $\Pi_{\mathcal{T}}$ in the collection of planes in \mathbb{H}^3 corresponding to $f(\mathcal{T})$. This plane is stabilized by a copy of the fundamental group of some turnover (possibly a smaller turnover that is covered by $f(\mathcal{T})$, if the fundamental group of $f(\mathcal{T})$ is not maximal)—a subgroup Γ of isometries of the fundamental group of the orbifold \mathcal{O}_T —for which there is a tiling of $\Pi_{\mathcal{T}}$ by hyperbolic triangles whose edges are a (possibly proper) subset of the intersections of $\Pi_{\mathcal{T}}$ with Γ -translates of the faces of T , and whose vertices are a (possibly proper) subset of the perpendicular intersections of $\Pi_{\mathcal{T}}$ with Γ -translates of the edges of T . We will locate all of the immersed turnovers in \mathcal{O}_T by reversing this process, that is, by determining exactly the hyperbolic planes in the universal cover \mathbb{H}^3 that are stabilized by a triangle subgroup of $\pi_1(\mathcal{O}_T)$. We therefore choose an arbitrary edge e_1 of T and develop copies of T in \mathbb{H}^3 (by reflecting in faces) until we find another edge e_2 which is coplanar with but which shares no (generalized) vertex with e_1 . The common plane, which we denote by Π_F (where F is a face of T incident to e_1), should consist of developed faces of T . Let Π_1 be the plane containing another face of T incident with e_1 , and let Π_2 be the plane containing another face of (a developed image of) T containing e_2 . Suppose that Π_1 and Π_2 intersect Π_F at angles of π/a and π/b , respectively. If Π_1 and Π_2 intersect at an angle of π/c , and if $1/a + 1/b + 1/c < 1$, then the rotations about edges e_1 and e_2 (of orders a and b , respectively), will generate a triangle subgroup of $\pi_1(\mathcal{O}_T)$, and the invariant plane for that subgroup will project to an immersed turnover in \mathcal{O}_T (every developed edge of T that intersects the invariant plane for this triangle subgroup at an oblique angle will correspond to an immersion of the turnover). This determines a maximal triangle subgroup of $\pi_1(\mathcal{O}_T)$, and the type of the corresponding immersed turnover will be (a, b, c) . Finally, we will show that, after sufficient development, there can be no such edge e_2 that is both coplanar with e_1 and that has an incident face whose corresponding plane Π_2 intersects the plane Π_1 . Thus, our determination of the immersed turnovers in \mathcal{O}_T will be complete.

We divide the remainder of the proof of Theorem 1.2 into subsections.

4.1. The case when a single edge separates e_1 from e_2 :

FIGURE 11. Part of the link of a non-finite vertex of $T[2, m, q; n, p, r]$

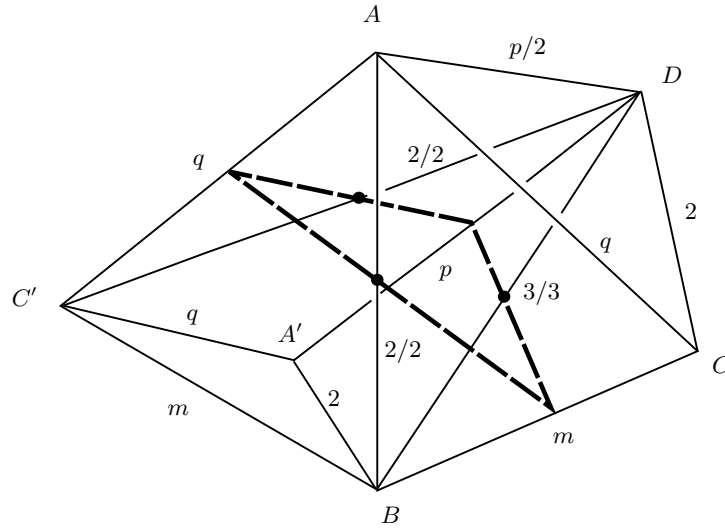
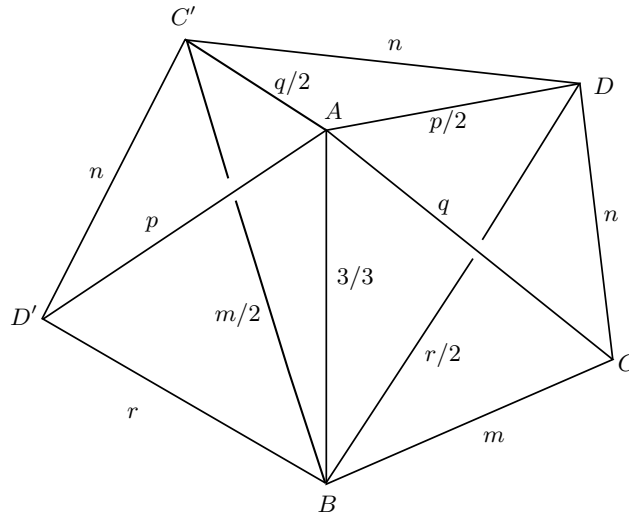
other angles in the figure refer to the measure at the appropriate triangular vertex). Using this inequality, we conclude that the indicated bold rays directed northwest from DA and DC do not intersect, because the sum of the angles that these rays make with the segment from DC to DA is at least π (and similarly for the rays directed southeast from DC' and DB , because the sum of the angles that these rays make with the segment from DB to DC' is at least π). Consequently, the bold lines in the figure (and the corresponding planes Π_1 and Π_2) cannot intersect in this case. A similar argument implying that Π_1 and Π_2 do not intersect holds when $n = 2$ and both p and r are greater than 3: The rays directed northwest from DA and DC make angles with the segment between these two points of $(p-2)\pi/p \geq \pi/2$ and $\pi/2$, respectively, and so the sum of these angles will be at least π (when $n = 2$ and $r \geq 4$, the same argument proves that the southeast rays from DC' and DB do not intersect). Finally, if $n = 2$ and $p = 3$ (respectively, $r = 3$), then it is easily seen Π_1 and Π_2 intersect at an angle of π/r (respectively, π/p), and the line of intersection passes through the point DB' (respectively, DA').

We therefore have, when $l = 2$ and our search for a turnover crosses only one edge, that an immersed turnover only arises when $n = 2$ and either $r = 3$ or $p = 3$. If $r = 3$, then this yields a triple of planes intersecting pairwise in angles of π/q , π/m and π/p ,

Supergroup	Subgroup	Index	Normal
$(3, 3, t)$	(t, t, t)	3	Yes
$(2, 3, 2t)$	(t, t, t)	6	Yes
$(2, s, 2t)$	(s, s, t)	2	Yes
$(2, 3, 7)$	$(7, 7, 7)$	24	No
$(2, 3, 7)$	$(2, 7, 7)$	9	No
$(2, 3, 7)$	$(3, 3, 7)$	8	No
$(2, 3, 8)$	$(4, 8, 8)$	12	No
$(2, 3, 8)$	$(3, 8, 8)$	10	No
$(2, 3, 9)$	$(9, 9, 9)$	12	No
$(2, 4, 5)$	$(4, 4, 5)$	6	No
$(2, 3, 4t)$	$(t, 4t, 4t)$	6	No
$(2, 4, 2t)$	$(t, 2t, 2t)$	4	No
$(2, 3, 3t)$	$(3, t, 3t)$	4	No
$(2, 3, 2t)$	$(2, t, 2t)$	3	No

TABLE 1. Triangle Supergroups and Subgroups

with $q \geq 3$, $m \geq 6$ and $p \geq 6$. If $p = 3$, then the pairwise angles of intersection are π/q , π/m and π/r , with $q \geq 6$, $m \geq 3$ and $r \geq 6$. (The inequalities are induced by the assumption that all of the vertices of T are non-finite.) By analyzing Table 1 (whose data is collected from Singerman [14]), we see that this triple of planes does not yield a triangle group that contains any other triangle group. By comparing the second column of the table with the first, we note that it is possible for this triple of planes to yield a triangle group that is contained in some larger triangle group. However, it is not possible for such a supergroup to be a subgroup of $\pi_1(\mathcal{O}_T)$. This follows from the observation in the paragraph following the proof of Theorem 1.3: Because such a supergroup would be a maximal triangle subgroup of $\pi_1(\mathcal{O}_T)$ stabilizing the plane that contains the (q, m, p) (or (q, m, r)) triangle, there would have to be edges in the development of T that intersect the interior of the (q, m, p) (or (q, m, r)) triangle perpendicularly (these intersections would be necessary for the corresponding orbifold covering of the smaller turnover by the larger (q, m, p) or (q, m, r) turnover). By construction, there are no such perpendicular intersections in the interior of the triangle. See Figure 12, which illustrates the case when $r = 3$. As can be seen in the figure, no developed edges of T intersect the interior of the (q, m, p) triangle (the intersections with this triangle that yield immersions of the corresponding turnover are indicated by the dots). Consequently, we can conclude that the (q, m, p) or (q, m, r) triangle determined by Π_1, Π_F and Π_2 is not parallel to any of the vertices of T , and therefore that it determines an immersed turnover in \mathcal{O}_T , because \mathcal{O}_T is small. The observations of this paragraph are summarized in items (1) and (2) at the conclusion of the paper.

FIGURE 12. A (q, m, p) triangle in $T[2, m, q; 2, p, 3]$ FIGURE 13. Three copies of the tetrahedron $T[3, m, q; n, p, r]$

4.1.2. *The single separating edge has order 3:* We next turn to the case in which the immersed turnover can be found after crossing only one edge between e_1 and e_2 , where the order of the crossed edge is $l = 3$. See Figure 13. Let $e_1 = AD'$, $e_2 = BC$, $\Pi_1 = AC'D'$ and $\Pi_2 = BCD$. We make several preliminary observations:

- (1) Any two (distinct) planes that truncate developed vertices will always be disjoint.

- (2) By (1) and by the fact that T has no finite vertices, any two developed edges of the tetrahedron (whose corresponding geodesics in \mathbb{H}^3 are distinct) will always be disjoint.
- (3) It is always the case that the plane containing one face of a generalized hyperbolic tetrahedron will be disjoint from the plane that truncates the vertex opposite to that face.
- (4) By (2), if two planes corresponding to two developed faces of T meet a third plane that corresponds to a developed face of T , then any intersection of the first two planes must occur on the side of the third plane where the two interior supplementary angles of intersection sum to less than π .
- (5) Any two planes corresponding to two developed faces that both intersect a third plane that truncates a developed vertex intersect if and only if their intersections with that truncated plane (i.e., with the link of the generalized vertex) do so. A corresponding statement is also true in the case when the developed vertex is ideal, that is, that two planes corresponding to two developed faces that intersect at infinity in the case of an ideal vertex intersect in \mathbb{H}^3 if and only if their intersections with the link of the ideal vertex themselves intersect.

Hence, by (3), we have that Π_2 is disjoint from the plane that truncates the vertex A . When $r = 2$, the planes Π_1 and Π_2 will intersect if and only if their intersections with the link of C' themselves intersect (by (4)). We will analyze the $r = 2$ case in a moment. When $r \geq 3$, we also have that Π_2 does not intersect the plane that truncates the vertex C' , reasoned as follows. We will always choose the “inward” normal direction for a plane that contains a face of T by indicating the appropriate opposite vertex to that face in any of our diagrams. When $r = 3$, we observe that Π_2 contains the face of the tetrahedron (not pictured in the figure) that is the reflection of $ABDC'$ through the face BDC' , and so Π_2 does not intersect the truncating plane of C' in this case (by (3)). When $r \geq 4$, then we consider the line containing the segment BD which divides Π_2 . The half of Π_2 that meets C is prevented from intersecting the truncating plane for C' by the plane ABD , and the other half of Π_2 is prevented from intersecting the truncating plane at C' by the plane containing the reflection of ABD through the face BDC' (both of these follow from (3)).

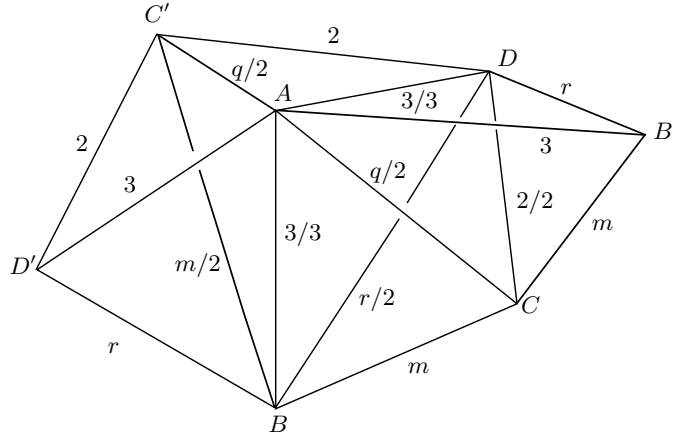
Therefore, when $r \neq 2$, we have that Π_2 has no intersection with the planes that truncate the vertices A and C' . We observe now that these truncating planes at A and C' determine an open ball (i.e., the region between them in \mathbb{H}^3) which contains Π_2 . We also note that the edge from A to C' is the only segment of the line of intersection of Π_1 with the planes ABC' and ADC' that lies in this ball. Using the convention for the inward normal direction given above, we conclude that, in order for Π_1 to intersect Π_2 , it is necessary for that intersection to occur on the *outward* side of either ABC' (where inward is relative to D) or the *outward* side of ADC' (where inward is relative to B), and consequently that Π_2 must cross at least one of the planes ABC' or ADC' .

By considering the geometry of the generalized vertex B , we have that Π_2 meets ABC' if and only if $r = 2$, and so we analyze this case now. In this case, $\Pi_2 = BDC'$ (as planes) and Π_1 and Π_2 intersect if and only if their intersections with the link of C' intersect (by (5)). The conditions for this intersection in the link of C' are either $m = 2$ (not possible, since $r = 2$), or $n = 2$ and one of q or m equals 3 (not possible, since $r = 2$), or else $q = 2$. In the last case, the intersection of Π_1 and Π_2 occurs along the edge $C'D$ at an angle of π/n , and because $q = 2 = r$ we must have $m \geq 6$, $p \geq 6$ and $n \geq 3$. In this case, $T = T[3, m, 2; n, p, 2]$ contains an immersed (m, n, p) turnover, and this tetrahedron (and the set of conditions on m, n and p) is isometric to the tetrahedron $T[2, p, n; 2, m, 3]$, which appears in item (1) at the end of the paper (it is listed as item (3), additionally). The summary at the end of the paper gives exact conditions on the arrangements of l, m, q, n, p and r which yield isometric tetrahedra.

Otherwise, we have that Π_2 must intersect ADC' , and any possible intersection of Π_1 and Π_2 must occur on the outward side of ADC' (that is, the side opposite to vertex B). Using the geometry of the generalized vertex D , we conclude that either $r = 2$ (the case we just analyzed), or $p = 2$, or $n = 2$ and one of p or r equals 3. If $p = 2$, then $q \geq 6$ (using the vertex A), $n \geq 3$ (using the vertex D), and $ADC' = ACDC'$ (as planes). By item (2) above, the lines AC' and CD are disjoint lines in the plane $ACDC'$. These lines are also the intersections with $ACDC'$ of Π_1 and Π_2 , respectively. We consider the side of $ACDC'$ that is outward from vertex B , and the interior angles of intersection $(q - 2)\pi/q$ (formed by Π_1 and $ACDC'$) and $(n - 1)\pi/n$ (formed by Π_2 and $ACDC'$) on this side of $ACDC'$ (that is, the two angles of intersection contained on this side of $ACDC'$ and in the same complementary component of these three planes). The conditions on n and p imply that $(n - 1)\pi/n + (q - 2)\pi/q \geq \pi$, and because it is only possible for Π_1 and Π_2 to intersect to the outward side of $ACDC'$ (relative to the inward B direction), we use item (4) above to conclude that $\Pi_1 \cap \Pi_2 = \emptyset$ in this case.

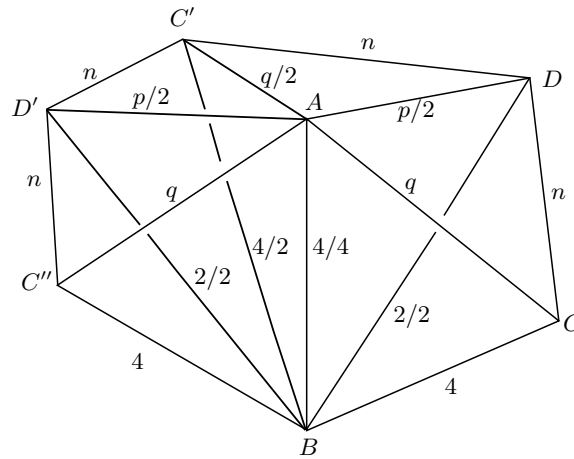
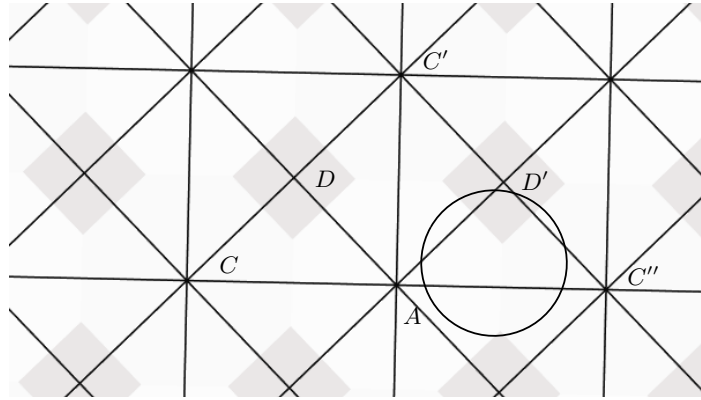
In the remaining case, we have $n = 2$ and one of p or r equals 3. If $p = 3$, then $r \geq 6$ and q and m must both be bigger than 2 and also satisfy $1/q + 1/m \leq 1/2$. We modify Figure 13 by adjoining another copy of T to the face ACD . See Figure 14. In this case, $ADC' = AB'DC'$ as planes, and we consider, as in the previous case, the interior angles of intersection $(q - 2)\pi/q \geq \pi/3$ and $(r - 1)\pi/r \geq 5\pi/6$ formed by $AB'DC'$ with Π_1 and Π_2 , respectively, on the outward side of this plane (again, relative to the inward B direction). Since $(r - 1)\pi/r + (q - 2)\pi/q > \pi$, and again because Π_1 and Π_2 can only intersect on the side of $AB'DC'$ opposite to B , we conclude that $\Pi_1 \cap \Pi_2 = \emptyset$ in this case. The case when $n = 2$ and $r = 3$ is entirely similar, with the same conclusion.

4.1.3. The single separating edge has order greater than 3: We now handle the analogous cases to the previous two cases, that is, when the search for an immersed turnover crosses a single edge between the planes Π_1 and Π_2 , and when $l > 3$ (we

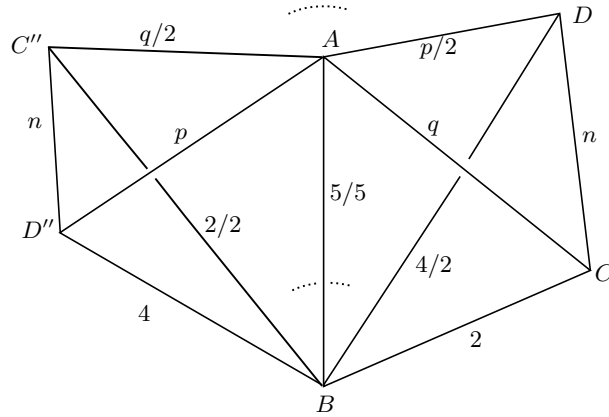
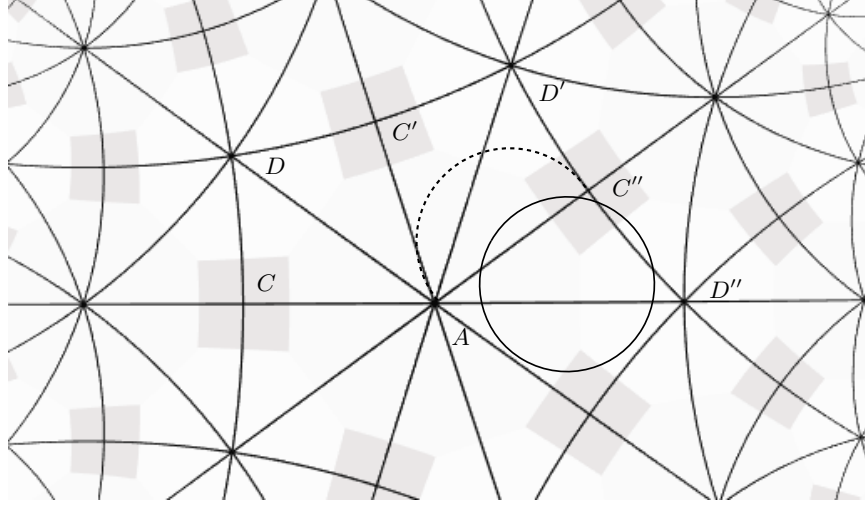
FIGURE 14. Four copies of the tetrahedron $T[3, m, q; 2, 3, r]$

will specify these planes in each example below, in an analogous way to the previous cases). We will show that no immersed turnovers can be found when $l > 3$.

We consider first the case when $l = 4$ and the vertex B has the Euclidean type $(2, 4, 4)$ with $m = 4$. See Figure 15. Referring to the lower half of this figure, we have $e_1 = AC''$, $\Pi_1 = AC''D'$, $e_2 = BC$ and $\Pi_2 = BCD$. The upper half of Figure 15 illustrates the view in the upper half-space model of \mathbb{H}^3 from the vertex B (which we have placed at the point at infinity). Now Π_2 is represented in this diagram by the line CD , and the plane Π_1 must be represented by a circle (the circle is the boundary of a hemisphere in this model of \mathbb{H}^3). We claim that the circle representing Π_1 must be centered at some point in the triangle $AC''D'$, and that none of the three points A , C'' or D' can be contained in this circle's interior. To see this, suppose first that the vertex A of the tetrahedron is a truncated vertex. Then the plane truncating that vertex would appear as a circle in the figure. This circle would have to be centered at the point labeled A because the geodesic edge from B to this plane must meet the plane perpendicularly. Next, we observe that the circle representing Π_1 must intersect the circle centered at A at a right angle (because Π_1 intersects the plane that truncates the vertex A perpendicularly). This is only possible if the point labeled A lies outside of the circle representing Π_1 . In the case when the vertex A of T is an ideal vertex, then the circle representing Π_1 would pass *through* the point labeled A . Since all of the vertices A , C'' and D' of the tetrahedron are non-finite, the circle representing Π_1 cannot contain the vertices of the triangle $AC''D'$ in its interior disk. Moreover, this circle must meet each line segment AD' , AC'' and $C''D'$ (at angles of π/p , π/q and π/n , respectively) and so the center of this circle must be contained in the triangle $AC''D'$. Such a circle is depicted. Since any such circle cannot intersect the line CD , we conclude that $\Pi_1 \cap \Pi_2 = \emptyset$. An analogous argument can be used to show that we obtain no immersed turnover in this fashion, whenever the vertex B is Euclidean and l is not equal to 2 or 3 (this occurs only when the triple (l, m, r) equals one of $(4, 2, 4)$, $(6, 2, 3)$ or $(6, 3, 2)$).

FIGURE 15. The view from the ideal vertex of type $(2, 4, 4)$.

We are left then to consider the case when $l \geq 4$ and the vertex B has a hyperbolic type. The argument is similar to the Euclidean vertex case, but we provide the details. Consider first the case of Figure 16 (the upper part of this figure, along with the similar figures in this section, was generated using the software *KaleidoTile* by Jeffrey Weeks [19].) For the purposes of illustration, we have assumed that the vertex B has the type $(2, 4, 5)$, with $l = 5$, $m = 2$ and $r = 4$. Here, we have $e_1 = AD''$, $\Pi_1 = AD''C''$, $e_2 = BC$ and $\Pi_2 = BCD$. We consider the hyperbolic plane Π_B that truncates vertex B as a hemisphere in the upper half-plane model, and wish to construct a “view from B ” that is similar to the previous case when the B was an ideal vertex. The Poincaré disk $(2, 4, 5)$ tiling pattern of the figure results from projecting this *hemisphere* to the bounding plane of \mathbb{H}^3 through the south pole of the *whole* sphere that contains it [17, Figure 2.12, p. 58]. An important observation about this projection is that it is equivalent to projecting every point $x \in \Pi_B$ to the bounding plane of half-space along the geodesic ray that is perpendicular to Π_B at x .

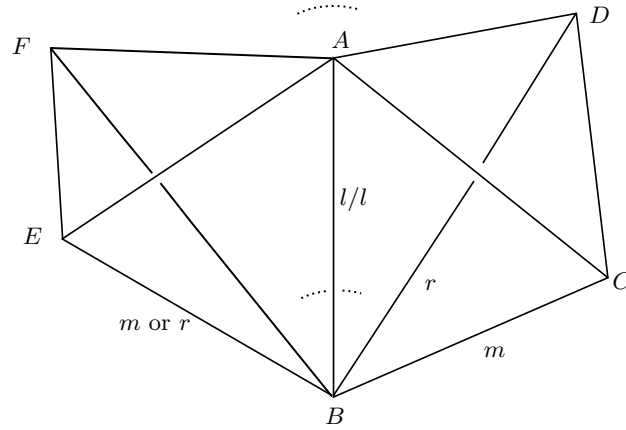
FIGURE 16. The view from the truncated vertex of type $(2, 4, 5)$.

In particular, as in the Euclidean vertex case, each line or circular arc in the figure is the ideal boundary of a plane (each plane corresponding to a face in the tiling of \mathbb{H}^3 by T) that meets Π_B perpendicularly, and this projection is conformal, so that the angle of intersection between two lines or circular arcs in the figure is equal to the angle of intersection of the corresponding planes in \mathbb{H}^3 . We have indicated, in the projection of the figure, the images of the intersection of five copies of T with Π_B , labeled the endpoints of the lines emanating from B by the corresponding letters in the lower part of the figure, and applied an isometry so that A (or, in the case that the vertex A is truncated, the center of the circle that represents the truncating plane for the vertex A) is at the center of the Poincaré disk. The planes Π_1 and Π_2 are represented by a circle and the circular arc CD , respectively. We observe that, if the vertex C'' is truncated, then the truncating plane $\Pi_{C''}$ for C'' will appear in the figure

as a circle (not pictured) with center on the segment AC'' , because the point labeled C'' is the endpoint of a semicircle in the half-space model that is perpendicular to both Π_B and $\Pi_{C''}$ (to see this, recall that we may consider the projection from Π_B to the bounding plane as a projection along arcs of such semicircles). As in the previous case, the point C'' cannot be contained in the interior of the circle that is the ideal boundary of Π_1 , because then the arc of the semicircle from C'' to its inverse image in Π_B under the projection would meet Π_1 , and this is impossible because this arc meets $\Pi_{C''}$ perpendicularly and $\Pi_{C''}$ and Π_1 are orthogonal (the contradiction arises because it would imply the existence of a triangle with two right angles). The same argument holds when either of A or D'' is a truncated vertex, and therefore, as in the previous case, we have that the ideal boundary of Π_1 must bound a disk whose interior is disjoint from the points A , C'' and D'' (these points may lie on the ideal boundary of Π_1 if they are ideal vertices of T). The ideal boundary of Π_1 intersects the segments AC'' and AD'' and the circular arc $C''D''$ at angles of π/q , π/p and π/n , respectively, and the center of the circle representing this ideal boundary has its center contained in the hyperbolic triangle $AC''D''$ in the projection. This is the circle that is depicted in the figure. But such a circle can have no points in the hyperbolic polygon $CAD''C''D'C'D$ that lie outside of the union of hyperbolic triangle $AC''D''$ and the circle with the segment AC'' as its diameter (pictured with a dashed arc in the figure). Consequently, this circle cannot meet any of the sides of this hyperbolic polygon other than AD'' and $D''C''$, and, in particular, we have $\Pi_1 \cap \Pi_2 = \emptyset$. An analogous argument works whenever B has hyperbolic type with one incident order 2 edge and $l \geq 4$.

The case when $l \geq 4$ and B has hyperbolic type with no incident order 2 edge is similar. See Figure 17, in which Π_2 is represented by the circular arc CD and Π_1 is represented as the circle pictured. When $l \geq 4$, we observe that, in any similar picture (for example, Figure 18), the angles $\alpha = (l - 2)\pi/l$ and $\beta = (r - 1)\pi/r$ will always be at least $\pi/2$. Consequently, since $\alpha \geq \pi/2$ and because the center of the circle representing Π_1 is contained in the hyperbolic triangle AEF , this circle will be disjoint from the interior of the segment AD (it may pass through A , if the corresponding vertex is ideal). Also, noting that AD will always have Euclidean length equal to one of the lengths $|AF|$ or $|AE|$, the conditions on α and β imply that no point of the circle CD that lies above the line AD will be closer to the center of the circle representing Π_1 than any of the points A , E or F . Since A , E and F are not contained in the interior of this circle, we can conclude that $\Pi_1 \cap \Pi_2 = \emptyset$ in this case.

4.2. The case when multiple edges separates e_1 from e_2 : Recall that $\Pi_{\mathcal{T}}$ denotes the plane stabilized by a copy of a triangle subgroup in the fundamental group of \mathcal{O}_T , and that e_1 and e_2 denote two developed coplanar edges of T whose (perpendicular) intersections with $\Pi_{\mathcal{T}}$ correspond to two of the cone points of an immersed turnover (whose fundamental group is the triangle group stabilizing $\Pi_{\mathcal{T}}$) in \mathcal{O}_T .



Notation. For the remainder of the paper, Π_F refers to the plane containing e_1 and e_2 . It is the development in \mathbb{H}^3 of one face F of T . The diagrams from Figures 19, 20 and 21 (along with several other figures later in this section) are all drawn with the convention that Π_F is the page containing the illustration. We use L_F to denote the intersection of $\Pi_{\mathcal{T}}$ with Π_F . Additionally, the phrase “the other side of Π_F ” refers, in each of the relevant figures, to the side of Π_F that is behind the page (relative to the reader), and the use of the word “plane” at any edge in a diagram *always* refers to a plane that the development of a face of T in \mathbb{H}^3 that passes through that edge.

Now that we have determined the conditions on T which give rise to a turnover in \mathcal{O}_T when $\Pi_{\mathcal{T}}$ intersects a single edge in the development of F between e_1 and e_2 , we will show that it is impossible for there to be more than one such edge in

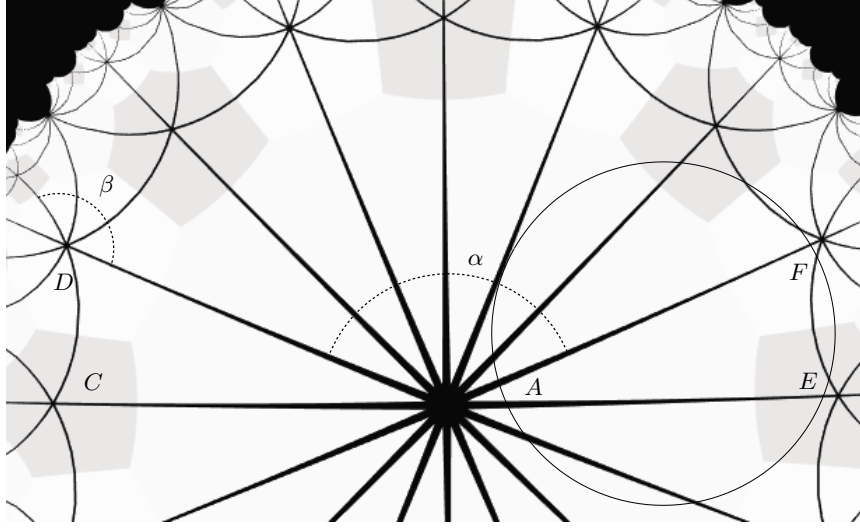


FIGURE 18. Another view from the truncated vertex of generic hyperbolic type when none of l , m and r is 2.

the development of F between e_1 and e_2 . This will complete the classification of immersed turnovers in tetrahedral orbifolds with no finite generalized vertices.

Figure 19 shows two possible schematic diagrams for this discussion. In each of the subfigures, the edges e_1 and e_2 are indicated, and the dotted line represents L_F . Notice that, in each triangle of the planar development of F , there is always a unique translate of a vertex of T that is separated from the other two by Π_T . The edge translates of T labeled by “ s ” represent points at which this vertex switches. We consider the following procedure for dividing any diagram of the type from Figure 19 into subdiagrams of the type (up to possible reflection or order two rotation) given in Figures 20 and 21:

- (1) Starting at the first edge of the diagram, we follow L_F until we arrive at the first switch. There must always be such a switch, for otherwise the supposed turnover would be parallel to a cover of an embedded turnover corresponding to one of the truncated vertices of T .
- (2) If the switch is the only switch in the diagram, then our diagram looks like, up to reflection or rotation, one of the diagrams from Figure 20. In this case, we stop.
- (3) If there is more than one switch and the diagram looks like, up to reflection or rotation, one of the diagrams from Figure 21, then we stop.
- (4) If we have not halted in the previous two steps, then the diagram up to and including the first edge after the first switch looks like the diagram in either Figure 20(a) or 20(b). Call this portion a *subdiagram*.
- (5) Starting at the last edge of the subdiagram from the previous step, we repeat this process with the remaining portion of the original diagram, starting from the first step, until we reach edge e_2 .

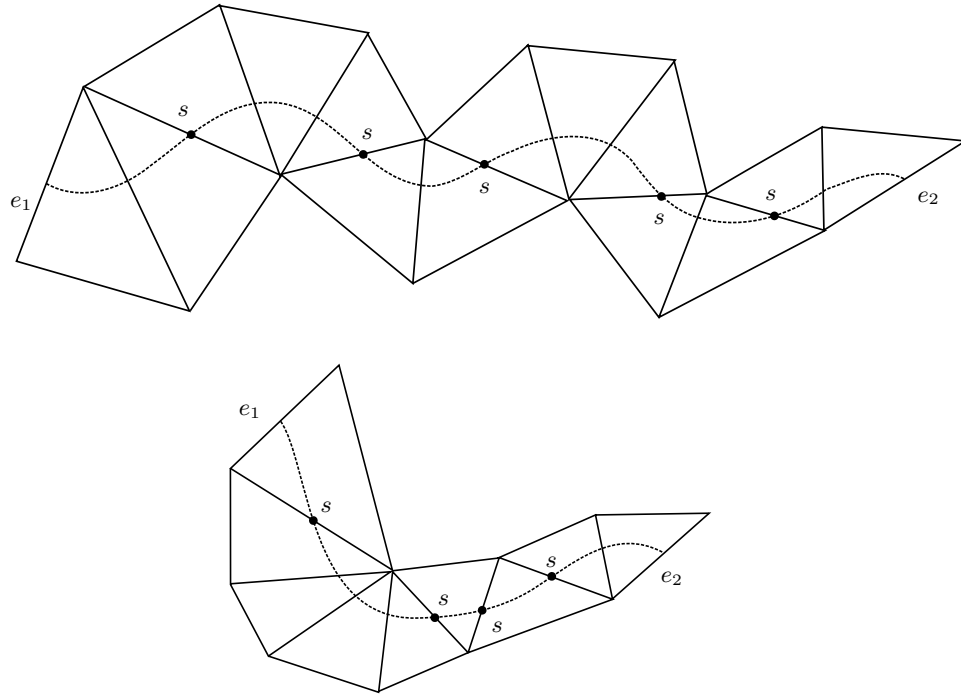


FIGURE 19. Schematic of some possible developments of a face of T , together with switches and the possible intersection of the plane $\Pi_{\mathcal{T}}$.

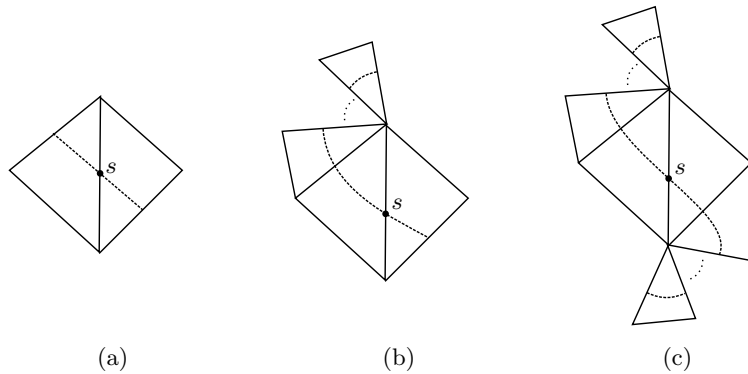


FIGURE 20. One type of possibility for the subdiagram components for a diagram of the type given in Figure 19.

This procedure divides our diagram into subdiagrams of the type illustrated in Figure 20(a) and 20(b), with the possible exception that the final subdiagram may be of the type in Figure 20(c) or one of the two types in Figure 21 (we note that this process can eliminate certain switches, in each of the resulting subdiagrams). Again, we denote by Π_1 and Π_2 the planes at e_1 and e_2 , respectively, whose intersections with $\Pi_{\mathcal{T}}$ are supposed to form two of the sides of a triangle in the tiling of $\Pi_{\mathcal{T}}$. Our strategy is to use the subdiagrams of Figures 20 and 21 to find a sequence of planes in \mathbb{H}^3 —one

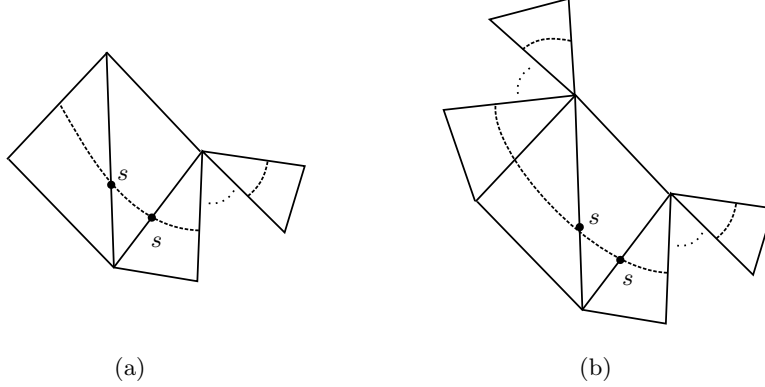


FIGURE 21. Another type of possibility for the subdiagram components for a diagram of the type given in Figure 19.

or more planes at each of the two outer-most edges of each subdiagram—that are pairwise disjoint on either side of Π_F and that therefore separate Π_1 from Π_2 .

We first make two observations about the subdiagram from Figure 20(a). First, if either of the orders of the two edges separated by the switch is 2, then no plane at either edge can meet any of the planes at the other edge (excepting the plane Π_F). This fact follows from the extensive analysis done in Subsection 4.1. Second, if the two planes at the outer edges that are inclined closest toward the switch (“inclined closest” means closest, on the other side of Π_F , to the planes that pass through the switch edge) do meet (thus generating an immersed turnover in \mathcal{O}_T with two singular points of order at least 6 and one singular point of order at least 3), then the next two planes (one at either outer edge) inclined away from the switch do not meet. This fact follows from an easy analysis of the patterns of line intersections in hyperbolic triangular tilings. See Figure 22 for the conditions on the vertex orders of an (a, b, c) hyperbolic triangular tiling under which such intersections can occur (in particular, one of the vertices must have order 2, which does not happen in this situation).

Therefore, it is left to show that, for each of the remaining types of subdiagram, the two planes at the outer-most edges that are inclined closest to the single or double switch in the subdiagram do not intersect (again, “inclined closest” means closest, on the other side of Π_F , to the planes passing through the switch edge(s)). This will produce the sequence of planes that separates Π_1 and Π_2 , and therefore complete the proof. We will show this by cases, which are indicated by their labels in the figures.

4.2.1. *20(b)*: See Figure 23, in which we have supposed without loss of generality that F is the face ABC of the tetrahedron T , as in Figure 9. This picture only differs from Figure 20(b) by a 180° rotation. Observe that the edges incident at the vertices A and B have orders l, q, p and l, m, r (respectively).

We observe that the vertex B must have at least one order 2 edge incident to it. Otherwise, if B were of the type (x, y, z) with all orders at least 3, then it is readily seen, by using the information from Figure 22(iii), that Π_2 (the plane through e_2

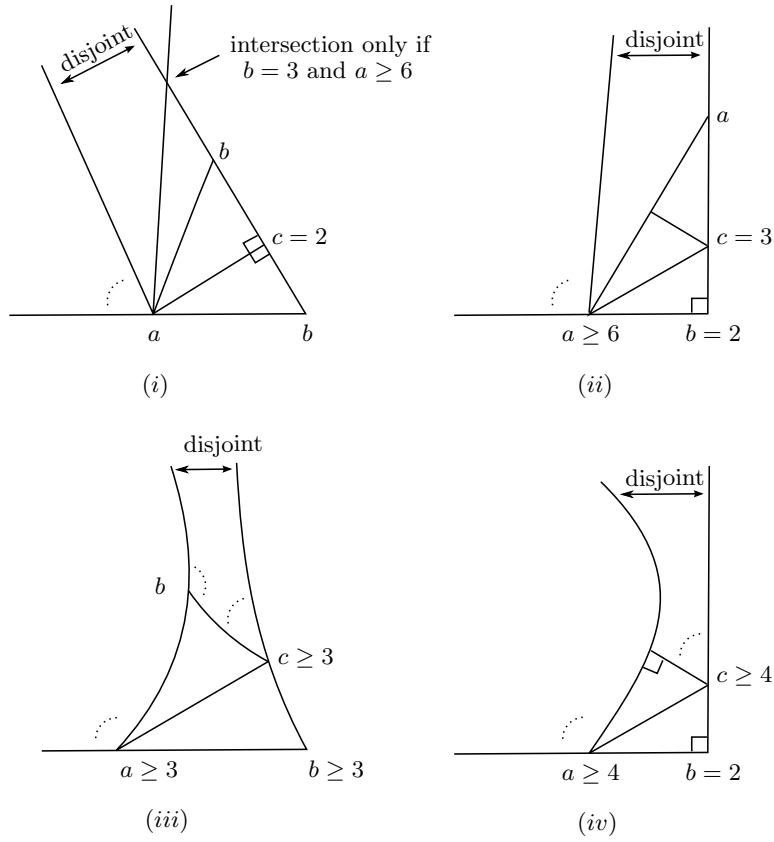


FIGURE 22. The possibilities for the intersection of lines in a triangular tiling of \mathbb{E}^2 or \mathbb{H}^2 .

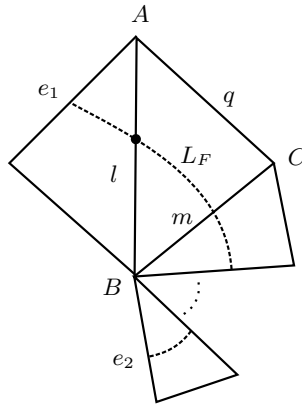


FIGURE 23. The case of Figure 20(b).

that is inclined closest to the switch) cannot meet the plane at edge BC that is inclined closest to the switch. We indicate how this can be determined. Recall that we may construct the view from B as a triangular tiling of either the Euclidean or

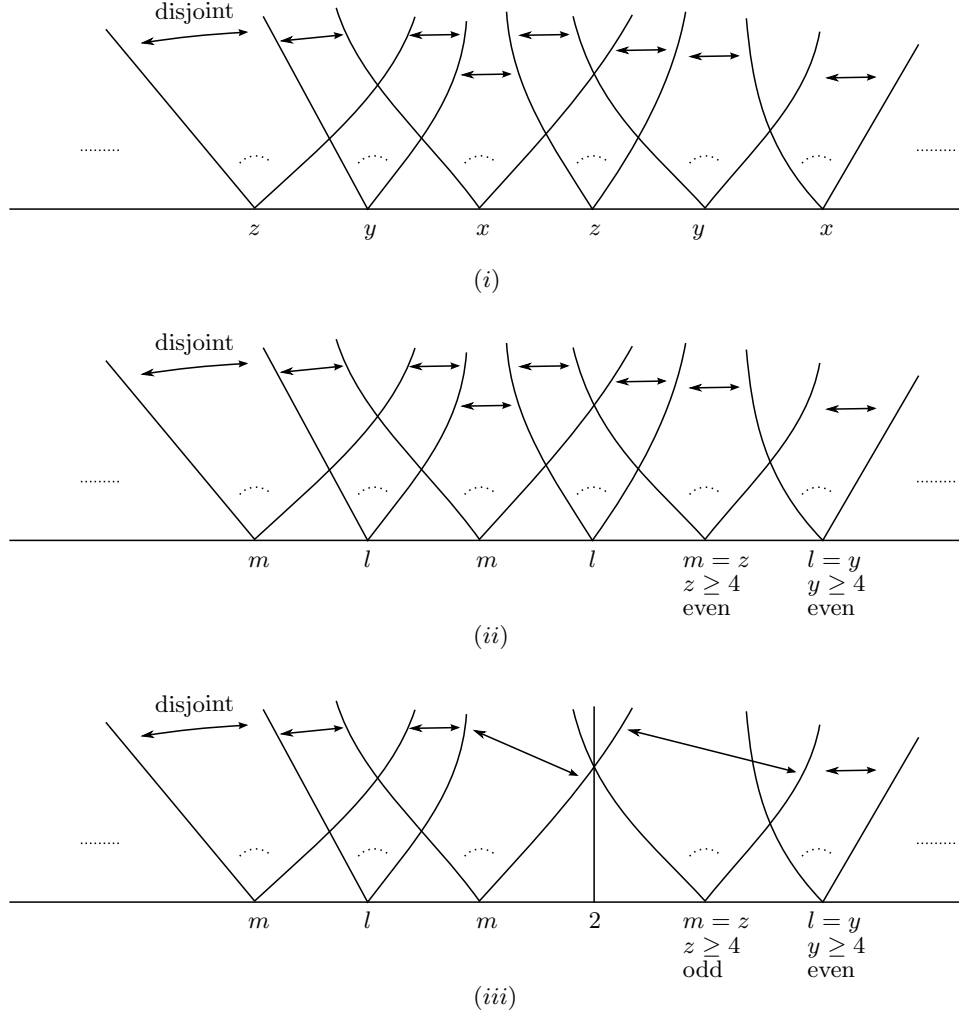


FIGURE 24. Patterns of intersections of certain lines corresponding to sides in a triangular tiling of \mathbb{H}^2 or \mathbb{E}^2 . Double arrows indicate two lines that do not intersect above the horizontal line.

hyperbolic plane (in this case, a tiling by (x, y, z) triangles) such that Π_F appears as a horizontal line, and such that each edge incident to B appears as a point on that line and each plane through an edge incident to B appears as a line (or hyperbolic line, if B is super-ideal) passing through the corresponding point in the view from B . Using Figure22(iii), we can conclude that the view from B , when B has no incident order 2 edge, looks schematically like Figure 24(i). This figure assumes that x , y and z are all odd; the other cases are similar. Suppose, for example, that the right-most point x in this figure represents the edge BC (x also indicates the order of that edge), and that the (schematic) line through this point inclined furthest to the right represents the plane through edge BC inclined closest to the switch edge AB . Then it is easily seen that no right-most inclined line through any subsequent point to the left along

the horizontal can intersect with this line. Consequently, the planes to which these lines correspond cannot intersect on the other side of Π_F (i.e., the other side of the page in Figure 23). In particular, Π_2 cannot cross the plane through BC inclined closest to the switch, as we wished to show. Furthermore, by our analysis in the cases of Subsection 4.1, the only way that Π_1 can meet the plane through edge BC that is inclined closest to the switch is if B has an incident order 2 edge. Consequently, if there is no such order 2 edge at B , then we have $\Pi_1 \cap \Pi_2 = \emptyset$.

So B either has the type $(2, 3, x \geq 6)$ or $(2, y \geq 4, z \geq 4)$. In the latter case, if $l = y$ or $l = z$, then we have shown in Subsection 4.1.3 that Π_1 is disjoint from every plane through edge BC . If $l = y$ and $m = z$ and l and m are both even, then it is a simple exercise, using Figure 22(i), to show that no plane that is inclined closest to the switch edge AB through any of the subsequent edges from BC toward e_2 along L_F can meet the plane through edge BC that is inclined closest to the switch, as in the argument of the previous paragraph (the schematic of the view from B in this case would be Figure 24(ii), with the edges AB and BC corresponding to the right-most points labeled l and m , respectively). So $\Pi_1 \cap \Pi_2 = \emptyset$ in this case. If $l = y$ and $m = z$ and m is odd, we can use the same argument (this time using the information from items (i), (ii) and (iv) from Figure 22 to obtain the schematic view from B as depicted in Figure 24(iii)) to conclude that $\Pi_1 \cap \Pi_2 = \emptyset$. The analogous cases, where $l = y$ and $m = z$ and l and m are of mixed parity, are similar. The case when $l = y$ or $l = z$ and $m = 2$ requires a bit more analysis. In this case, we use the geometry of the vertex A , the fact that $l \geq 4$ and the information from Figure 22 to conclude that Π_1 cannot intersect the plane through edge AB that is inclined closest to the edge BC . But Π_1 must intersect Π_F and it must intersect some of the planes through the switch edge AB . We refer to Figure 25, which depicts the schematic view from B in this case, with $l = y \geq 4$ and $m = 2$ (the third edge incident to B , which would have the label r in the tetrahedron T , is labeled by $z \geq 4$). In this figure, the line segment AD corresponds to the plane through the switch edge AB of the tetrahedron that is inclined closest to the edge BC . As we have seen in previous cases, the ideal boundary of Π_1 , in this view, is a circle that cannot contain any vertex of the triangulation in its interior disk. Since $z \geq 4$, we may conclude from the figure that the ideal boundary of Π_1 cannot intersect the line $A'D$. By noting that the line $A'D$ represents the plane inclined closest to the switch through the edge just after the edge BC along L_F toward e_2 in Figure 23, we may use the previous arguments from this paragraph to conclude that $\Pi_1 \cap \Pi_2 = \emptyset$ in this case.

Referring to the first sentence of the previous paragraph, in the latter case and when $l = 2$ and $y = 4 = z$, we may show that $\Pi_1 \cap \Pi_2 = \emptyset$ by using the Euclidean vertex argument as in Figure 15. In the latter case and when $l = 2$ and one of y or z is greater than 4, it is again readily shown that the second closest plane to the switch through edge BC (recall that Π_1 must be disjoint from this plane, by the observation of the penultimate paragraph before the start of this subsection) misses the plane inclined closest to the switch at every subsequent edge that L_F crosses toward e_2 .

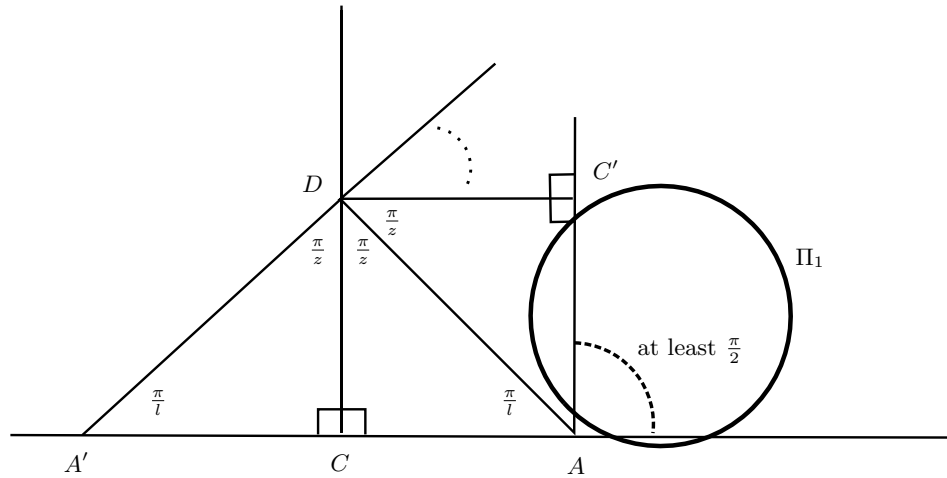


FIGURE 25. The schematic view from the vertex B in the case when $l = y \geq 4$, $m = 2$ and $r = z \geq 4$.

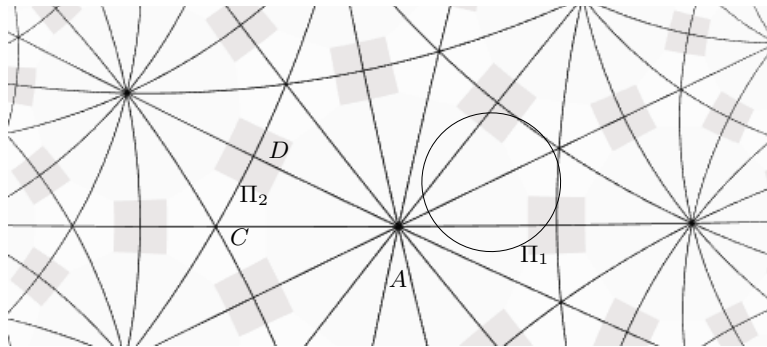


FIGURE 26. A view from the truncated vertex of hyperbolic type $(2, 3, 7)$.

The argument uses the information of items (i), (ii) and (iv) from Figure 22, and is similar to the arguments already presented in the previous two paragraphs. Thus, we have $\Pi_1 \cap \Pi_2 = \emptyset$ in the case that the type of vertex B is $(2, y \geq 4, z \geq 4)$.

This leaves us with the possibility that B has type $(2, 3, x \geq 6)$. When $l = x$, then we are in a case that is similar to the first case in Section 4.1.3, i.e., we have to consider a regular l -gon in either the Euclidean or hyperbolic plane and a circle centered inside the polygon that does not contain in its interior the center of the polygon, any vertex of the polygon or any midpoint of a side. In this case, however, we observed that such a circle (representing Π_1) must be disjoint from all but two sides of the polygon. But the plane Π_2 will correspond in such a picture to a line or circular arc in the picture that does not meet the interior of this polygon, and so $\Pi_1 \cap \Pi_2 = \emptyset$ when $l = x$. See Figure 26 for an example illustration of this argument, in the case when $x = 7$.

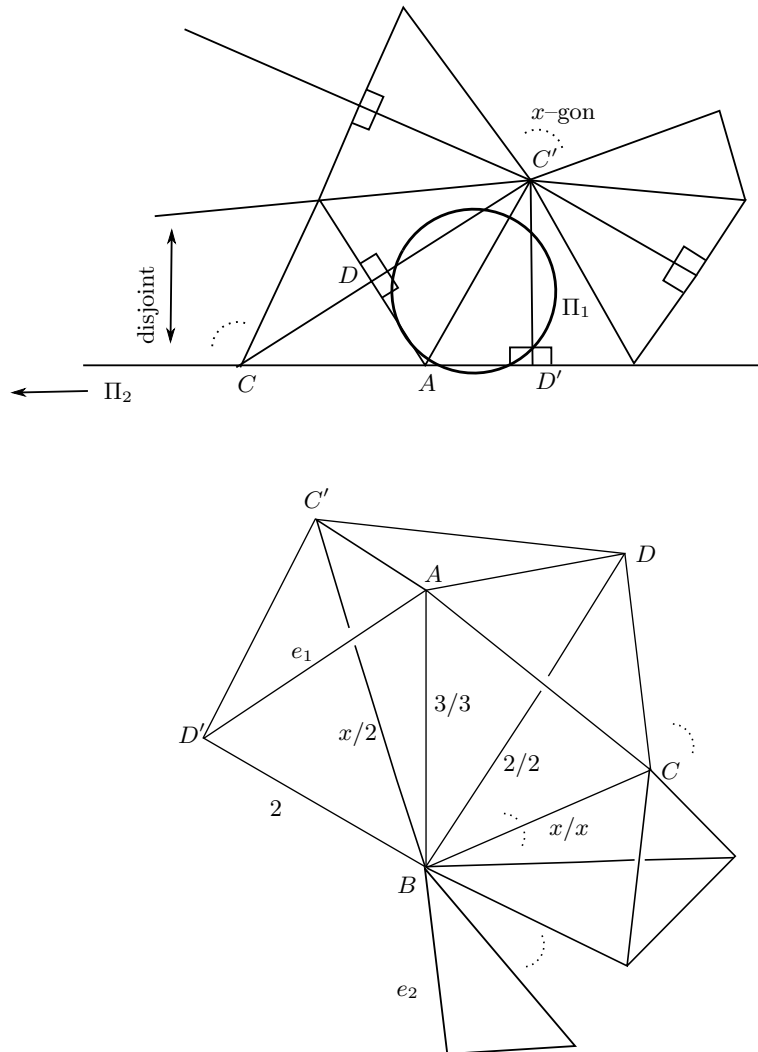
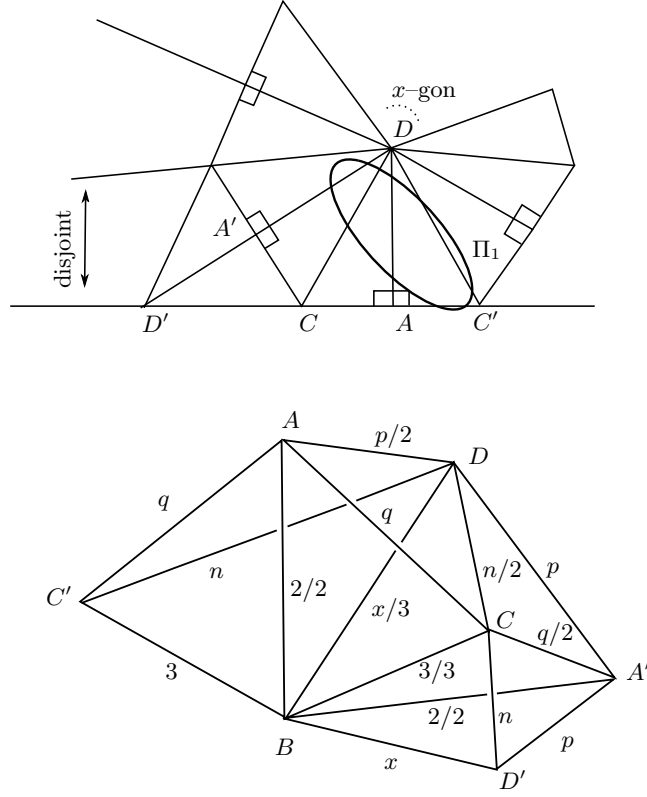


FIGURE 27. A view from the truncated vertex of type $(2, 3, x \geq 6)$.

The cases when $l = 2$ or $l = 3$ remain. In the case when $l = 3$, we refer to Figure 27. The upper half of this figure depicts the salient aspects of the view from vertex B , as in the previous cases we have considered. The lower half of the figure depicts part of the development of T in \mathbb{H}^3 . In particular, in the lower half of the figure, the triangle with edge e_2 and the lowest set of elliptical dots are both meant to lie in Π_F (which is the horizontal line CAD' in the upper half of the figure), and the plane Π_2 is not depicted, although $\Pi_1 = AC'D'$ is. In the upper half of the figure, Π_1 is represented by a circle centered at some point inside the triangle $AC'D'$ that cannot meet any vertex of the triangulation and that can only meet the sides AD and AD' of the x -gon centered at C' (the fact that this circle can meet no other sides of the x -gon centered at C' follows by an argument similar to that depicted in Figure 16

FIGURE 28. A view from the truncated vertex of type $(2, 3, x \geq 6)$.

from Section 4.1.3). Since Π_2 must be represented by a line emanating from a vertex on the line CAD' which is further to the left than C (the direction, in the upper part of the figure, to which the line representing Π_2 must lie is indicated by the lower left arrow), and no such lines will enter the x -gon centered at C' , we conclude that $\Pi_1 \cap \Pi_2 = \emptyset$ in this case.

When $l = 2$, then the only way for which we are unable to apply the preceding argument is when $m = 3$. See Figure 28. This is because the angle $\angle A'DC'$ is less than $\pi/2$ when $x > 6$, and so it is, in principle, possible that the circle representing Π_1 (whose center must be contained in the triangle $AC'D$) may intersect the line representing Π_2 if the latter is the line $A'D'$ (we have drawn the circle as an ellipse in order to indicate this possible intersection). However, using the accompanying tetrahedral illustration and the techniques of Subsection 4.1 (applied to vertex D), it is readily seen that we must have $p = 2$ and $n = 3$ in order for Π_1 and Π_2 to intersect. However, because we assume that T has no finite vertices and because $l = 2$, we do not allow $p = 2$. (Note: When $l = p = 2$ and $m = n = 3$ (so that the vertex A is finite), there is an immersed turnover is of type (q, x, x) in T , provided that $q \geq 3$ and $x \geq 4$. See the conjectural classification at the end of this paper. In our case, $T = T[2, 3, q; 3, 2, x]$, which is isometric to the tetrahedron listed in item (6).)

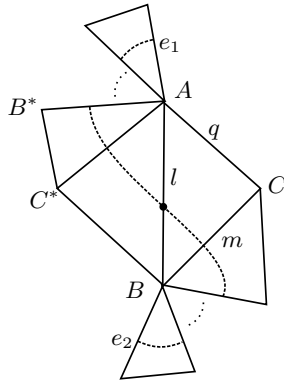


FIGURE 29. The case of Figure 20(c).

4.2.2. *20(c)*: See Figure 29, in which again we have supposed without loss of generality that F is the face ABC of the tetrahedron T , with the edges incident at the vertices A and B having orders l, q, p and l, m, r (respectively). We again denote by Π_1 and Π_2 the planes at the edges e_1 and e_2 , respectively, that are inclined closest to the switch edge. The dotted curve in all of these figures, which we denote by L_F , represents the intersection of the planar development Π_F of F with the plane that (purportedly) contains the turnover determined by Π_F , Π_1 and Π_2 .

Remark 3. The symbol “*” attached to a letter in this figure and in all subsequent figures is meant to indicate an ambiguity that may arise due to parity, and it is important for us to take note of it. For example, in Figure 29, if the order of the edge AB is even, then the vertex C^* is a developed copy of the vertex C , and the order of the edge AC^* is also q , i.e., the order of edge AC . However, if l is odd, then it would take an odd number l of tetrahedra developed around the edge AB to continue the development of the face ABC , making C^* a developed copy of the vertex D (recall that, behind the page, relative to the reader, lies the fourth vertex D of the tetrahedron), and making the order of the edge AC^* equal to p , i.e., the order of the edge AD (recall the notation $T[l, m, q; n, p, r]$ defined in Figure 9). We will avoid this notation whenever it is possible, although it will be necessary at times.

By the previous case, we know that Π_1 meets none of the planes through edge BC . It is therefore necessary, if Π_1 and Π_2 are to intersect, that Π_2 cross every plane through edge BC . As in the previous case, then, we can conclude that one of the edges incident at B must have order 2, for otherwise it is not possible for Π_2 to cross the plane through BC inclined closest to the switch.

Using Figure 22 and the fact that B must have an incident order 2 edge, we can reduce the cases that must be considered to those listed in Figure 30. We indicate how to achieve this reduction presently. Referring to Figure 29, suppose first that $l = 2$ and $m = 3$. Recall that the dotted curve represents the line L_F . Then the next edge incident to B that L_F crosses after BC in the direction away from the switch should have order $x \geq 6$. A schematic of the view from B is pictured in Figure 31(i).

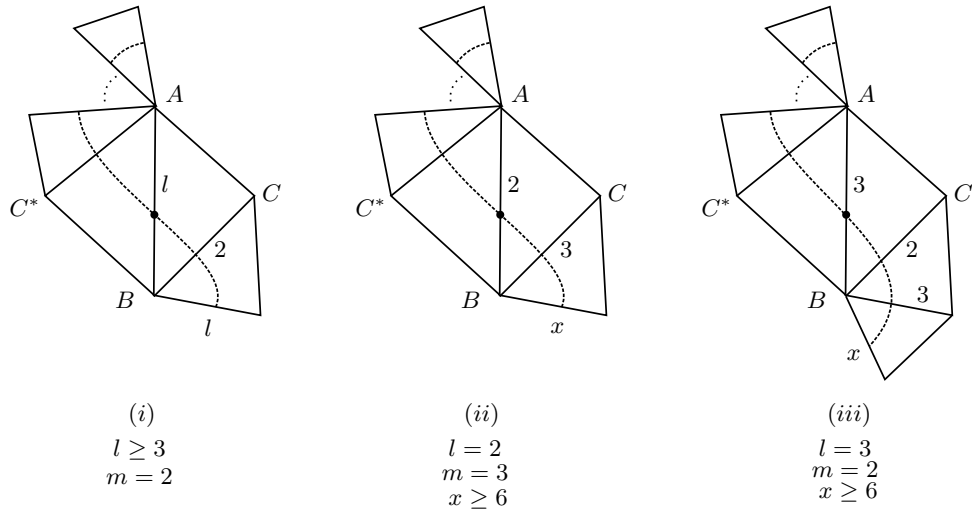
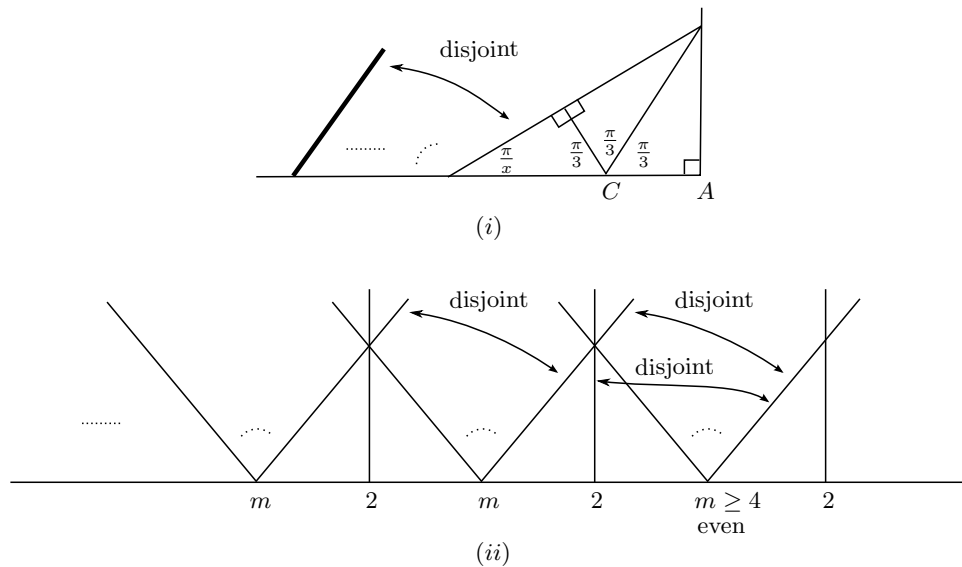


FIGURE 30. After analysis, the remaining cases of Figure 20(c).

FIGURE 31. Patterns of intersections of certain lines corresponding to sides in a triangular tiling of \mathbb{H}^2 or \mathbb{E}^2 . Double arrows indicate two lines that do not intersect above the horizontal line.

The bold line in the figure represents *any* plane through a subsequent edge incident to B that L_F crosses after the edge with order x . Because the angle α , which is formed by the bold line and the line AC , will always be at least π/x , we conclude that the two lines indicated in the figure by the endpoints of the double arrow will not intersect above the line AC . Consequently, because the line AC represents the plane Π_F , we conclude that the planes represented by these lines will not intersect on the other side of Π_F (recall that the other side of Π_F refers to the side underneath the

page in Figure 29. Therefore, we have reduced the case of showing that $\Pi_1 \cap \Pi_2 = \emptyset$ in Figure 29 to the case of subfigure (ii) in Figure 30, provided that $l = 2$ and $m = 3$. The case when $l = 2$ and m is even with $m \geq 4$ can be eliminated in an entirely similar fashion. See Figure 31(ii), which shows the pattern of intersections of lines that would result in the view from B . Here, we consider the right-most point on the horizontal (the horizontal represents Π_F in the view from B) with the label 2 as corresponding to the edge AB , and the right-most point on the horizontal with the label m as corresponding to the edge BC . It is readily seen from the figure that no lines passing through the labeled points on the horizontal to the left of the right-most point labeled m ever intersect the line through the latter point that is inclined closest to the switch point (i.e., the right-most point labeled 2). Therefore, no plane through an edge incident to B that is crossed by L_F after the edge BC can intersect the plane through BC inclined closest to the switch, when $l = 2$ and m is even and at least 4. So this case reduces to the previous case of Subsection 4.2.1, where it was shown that Π_1 has no intersection with the plane through BC inclined closest to the switch. In fact, all of the other reductions are arrived at in this way, that is, by using the information in Figure 22. The other cases that are *eliminated* by the methods of this paragraph are: (1) $l = 2$ and $m \geq 5$ with m odd, (2) $l = 3$ and $m \geq 6$ and (3) $l \geq 6$ and $m = 3$. The other cases that are *reduced* by the methods of this paragraph are: (4) $l \geq 3$ and $m = 2$ (which reduces to the case of Figure 30(i)) and (5) $l = 3$ and $m = 2$ (which reduces to the case of Figure 30(iii)). (We note that, when $l = 3$ and $m = 2$, case (i) of Figure 30 may seem to rule out case (iii). However, the plane inclined closest to the switch through the edge labeled x in case (iii) intersects the plane inclined closest to the switch through the lower edge labeled 3 (this may be seen using the information of Figure 22). We therefore must show that $\Pi_1 \cap \Pi_2 = \emptyset$ in *both* the case that e_2 is the lower edge labeled $l = 3$ in (i) *and* in the case that e_2 is the lower edge labeled x in (iii).)

Now, we apply the arguments of the previous two paragraphs to the other direction along L_F from the switch. Specifically, referring to Figure 29, we know by the previous case that Π_2 meets none of the planes through the edge AC^* , and so we reduce the possibilities for the number of developed faces around the vertex A using the fact that Π_1 must intersect every plane through the edge AC^* in order for it to be possible for Π_1 and Π_2 to have nonempty intersection. The result of this further analysis leaves us to consider only the cases of Figure 32. We note the change from “ $l \geq 3$ ” to “ $l \geq 3$ odd” that occurs when reducing Figure 30(i) to Figure 32(i). This change is due to the fact that, when l is even, the edge label “2” for AC^* in 32(i) must equal the edge label for AC . However, this would contradict our assumption that none of the vertices of T is finite, because C would have two incident edges, AC and BC , labeled 2.

So we are left to analyze the cases of Figure 32. We begin with case (iv). See Figure 33. The multiple parts of this figure are explained in the caption. Referring to the left side of the lower half of the figure, Π_1 is the plane through edge AC''' inclined

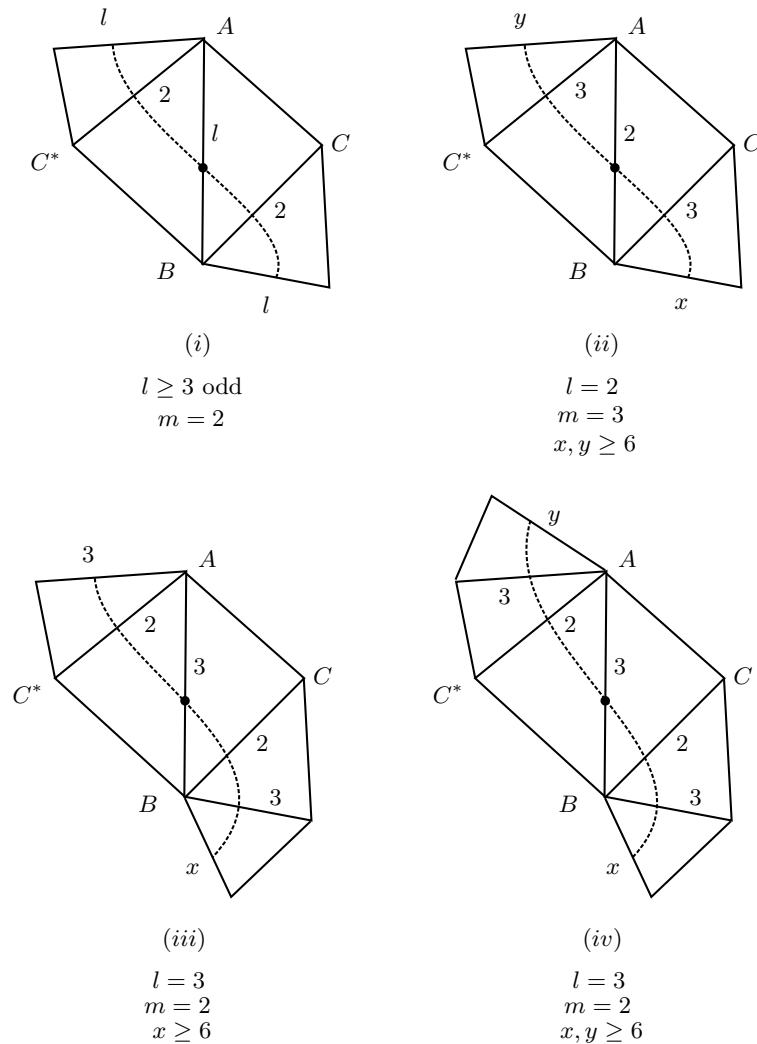
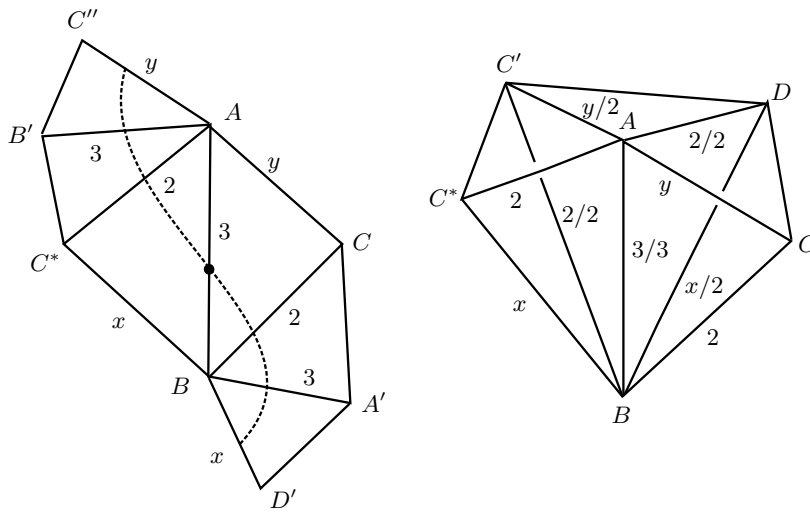
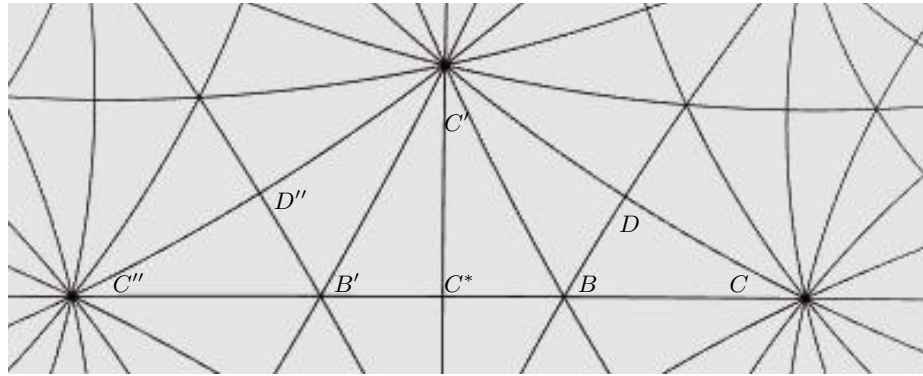


FIGURE 32. After further analysis, applied to the cases of Figure 30, these are the remaining cases of Figure 20(c) to consider.

closest to the switch edge AB and Π_2 is the plane through edge BD' inclined closest to the switch edge AB . We wish to show that $\Pi_1 \cap \Pi_2 = \emptyset$. We do so using the upper half of the figure, which shows the view from A under the assumption that $y = 7$ (the same argument we give here applies to any other value for $y \geq 6$). In the upper half of the figure, the plane Π_1 is represented by the line $C''D''$, and the plane ACD —which is depicted in the right side of the lower half of the figure, and which is the plane through AC inclined closest to the switch edge AB in the left side of the lower half of the figure—is represented by the line CD . Recalling that Π_F is the plane containing the face ABC (and, therefore, the plane in which the left side of the lower half of the figure is drawn, as well as the horizontal line in the upper half of the figure), we observe that there are two planes, other than Π_F , that pass through



$$\begin{aligned} l &= 3 \\ m &= 2 \\ x, y &\geq 6 \end{aligned}$$

FIGURE 33. The case of Figure 32(iv). The upper half of the figure represents the view from the vertex A when $y = 7$. The lower half consists of a perspective image of the three copies of the tetrahedron $ABCD$ on the right, and several triangles in the development of the face ABC on the left.

AB . These planes are represented in the upper half of the figure by the lines BC' and BD . Using the upper half of the figure, we observe that any point of Π_1 that is on the same side of ACD as the vertex B is also on the same side of the plane ABC' (which is represented by the line BC') as the point C^* . We now use the previous case (Section 4.2.1) to observe that $\Pi_2 \cap ACD = \emptyset$. Since Π_2 is on the same side of ACD as the vertex B , we conclude that any possible intersection of Π_1 and Π_2 must occur on the same side of the plane ABC' (depicted as the line BC' in the upper half of Figure 33) as the vertex C^* . But now an easy analysis (provided in the upcoming parenthetical) shows either that $ABC' \cap \Pi_2 = \emptyset$ and that the plane ABC' separates

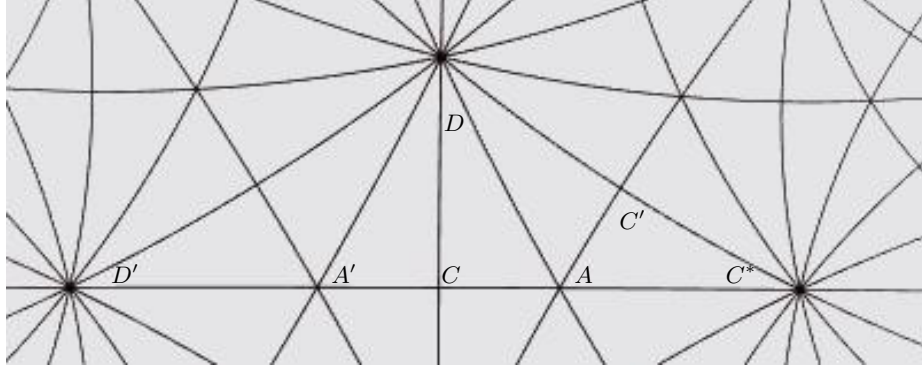


FIGURE 34. The view from the vertex B in the case of Figure 32(iv), when $x = 7$.

Π_2 from the vertex C^* , or that $ABC' \cap \Pi_2 \neq \emptyset$ and that any point of Π_2 that is on the same side of ABC' as C^* is on the *opposite* side of the plane $BC'C^*$ (pictured on the right side of the lower half of Figure 33) as the vertex A . Since, by the previous case (Section 4.2.1), we must have $\Pi_1 \cap BC'C^* = \emptyset$, and because Π_1 is on the *same* side of $BC'C^*$ as the vertex A , we conclude that $\Pi_1 \cap \Pi_2 = \emptyset$ in this case. (The analysis that proves the claim above about ABC' and Π_2 is as follows. Imagine the upper half of Figure 33 as the view from the vertex B , rather than A . Assume that $x = 7$ (the same argument holds for any $x \geq 6$), and replace C'' by D' , B' by A' , C^* by C , B by A , and C by C^* . Disregard the points labeled D'' , C' and D from the original figure. For the convenience of the reader, we provide Figure 34, which shows this relabeling along with the new positions (relative to B) of C' and D . Then in this new labeling, Π_2 is represented by the line $D'D$ and ABC' is represented by the line AC' . When $x \geq 7$, these lines either do not intersect, and the latter line separates the former from the point C^* . When $x = 6$, they do intersect, but they do so above the line $C'C^*$, which represents the side of the plane $BC'C^*$ opposite the vertex A .)

The argument of the previous paragraph can be used in case (iii) of Figure 32. See Figure 35. In the lower left half of this figure, Π_1 is the plane through the edge AB' inclined closest to the switch edge AB . In the lower right half, Π_1 is the plane $AC'B'A''$. In the upper half of the figure, which represents the view from A , Π_1 is represented as the line $B'C'$. Proceeding as in the previous paragraph, we have $\Pi_2 \cap ACD = \emptyset$ (by Section 4.2.1). If $x \geq 7$, we also know (by the parenthetical remarks at the end of the previous paragraph) that Π_2 is separated from the vertex C^* by the plane ABC' , and therefore, since the part of Π_1 on the side of ABC' opposite to vertex C^* is also on the side of ACD opposite to Π_2 , we have $\Pi_1 \cap \Pi_2 = \emptyset$. If $x = 6$, then we use the lower right part of Figure 35. By the parenthetical remarks at the end of the previous paragraph, we know that the part of Π_2 on the same side of ABC' as vertex C^* is also on the opposite side of the plane $BC'C^*$ from A . Therefore, if Π_1 (which is $AC'B' = AC'B'A''$ in the figure) does not intersect $BC'C^*$ at the vertex C' (that is, if the intersections of these two planes do not intersect in the link of C'), then Π_1 is never on the side of $BC'C^*$ that is opposite to vertex A ,

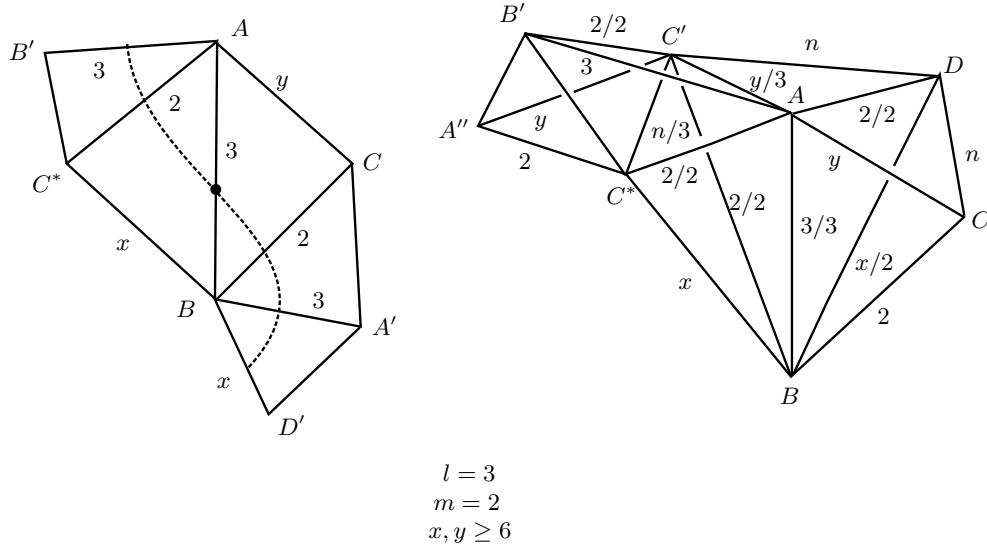
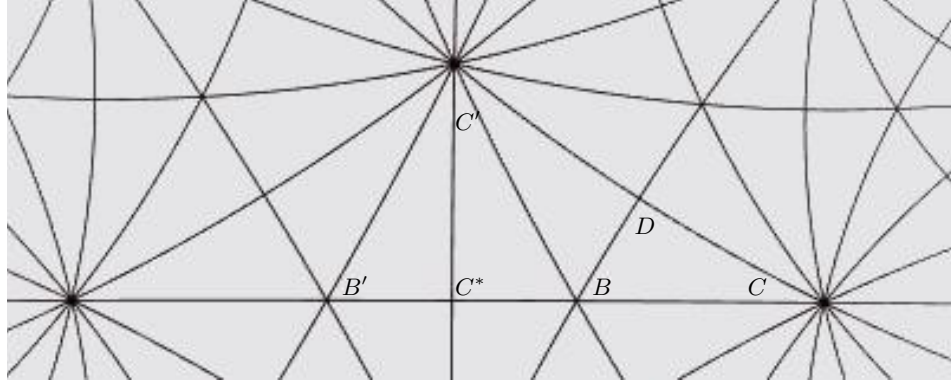


FIGURE 35. The case of Figure 32(iii). The upper half of the figure represents the view from vertex A . The right side of the lower half of the figure depicts the development of several copies of the tetrahedron, and the left side of the lower half depicts the development of the face ABC .

and we can conclude that $\Pi_1 \cap \Pi_2 = \emptyset$, because they do not intersect on either side of ABC' . Using the analysis of Section 4.1.1 applied to the two tetrahedra $AC'B'C^*$ and $ABC'C^*$, we conclude that Π_1 intersects $BC'C^*$ if and only if the edge CD of the tetrahedron has the label $n = 3$. In this case, however, we apply the techniques of Section 4.1.2. Specifically, we know that Π_1 and Π_2 can only intersect if they do so on the same side of $\Pi_F = ABC$ as D (because they form interior angles with Π_F of $\pi/3$ and $\pi/6$, respectively, on this side), on the same side of $ACD = ACDC'$ as B (because Π_2 lies entirely to this side of ACD), on the same side of $BDC'A''C^*$ as A (because they form interior angles of $\pi/y \leq \pi/7$ and $2\pi/3$, respectively, where

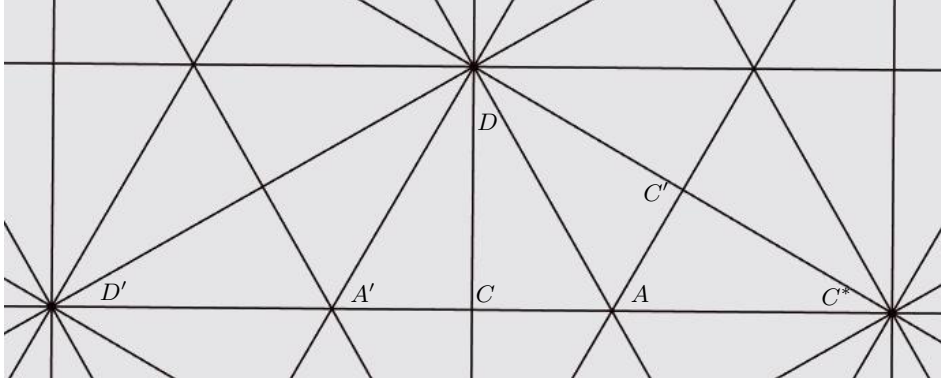


FIGURE 36. The view from the vertex B in the case of Figure 32(iii), when $x = 6$.

the latter angle is calculated using the view from B in Figure 36 as the angle at D between the lines $D'D$ and $C'D$, and on the same side of BCD as A (because Π_1 lies entirely to this side of BCD). The intersection of the half-spaces described in the previous sentence is depicted in the lower right part of Figure 35, and since it is clear that $\Pi_1 \cap \Pi_2 = \emptyset$ in this figure, we have finished the case of Figure 32(iii).

Turning to case (ii) of Figure 32, we employ an argument similar to, but much less intricate than, the argument of the previous two paragraphs. See Figure 37. Referring to the lower left of the figure, Π_1 is the plane through the edge AD' that is inclined closest to the switch edge AB , and similarly Π_2 is the plane through the edge BD'' inclined closest to AB . In the upper half of the figure (which is the view from A , as in the previous cases), Π_1 is represented by the line $D'D$. From the upper half of the figure, we know that the part of Π_1 on the same side of the plane ABD as the vertex C is also on the side of the plane ACD that is opposite vertex B . Using the symmetry of the figure, we know, similarly, that the part of Π_2 on the same side of ABD as the vertex C' is also on the side of the plane $BC'D$ that is opposite vertex A . Therefore, it is necessary to have $ACD \cap BC'D \neq \emptyset$ in order to have $\Pi_1 \cap \Pi_2 \neq \emptyset$. However, an easy analysis of the vertex D , using the techniques of Section 4.1.1, shows that $ACD \cap BC'D = \emptyset$, and so $\Pi_1 \cap \Pi_2 = \emptyset$ in the case of Figure 32(ii).

This leaves case (i) of Figure 32. We begin by assuming that $l \geq 5$ (recall that l must be odd). See Figure 38. The upper half of this figure depicts the view from the vertex A with the projection centered at the vertex B . For the purposes of illustration, we take the type of A to be $(2, 4, 5)$, although the argument only depends on the presence of the order 2 edge incident to A and the fact that the order of the edge is at least 5. The plane Π_1 is represented as the line $B'C^*$. We note that the plane $BC'D$ in the lower right part of the figure is represented in the upper half of the figure by a circle, centered on the line segment BC' because the planes $BC'D$ and ABC' are perpendicular, and whose interior disk does not contain any of the points B , D , C' or D' . As we have observed previously (among other places, in the argument depicted in Figure 16 from Section 4.1.3), the circle representing $BC'D$

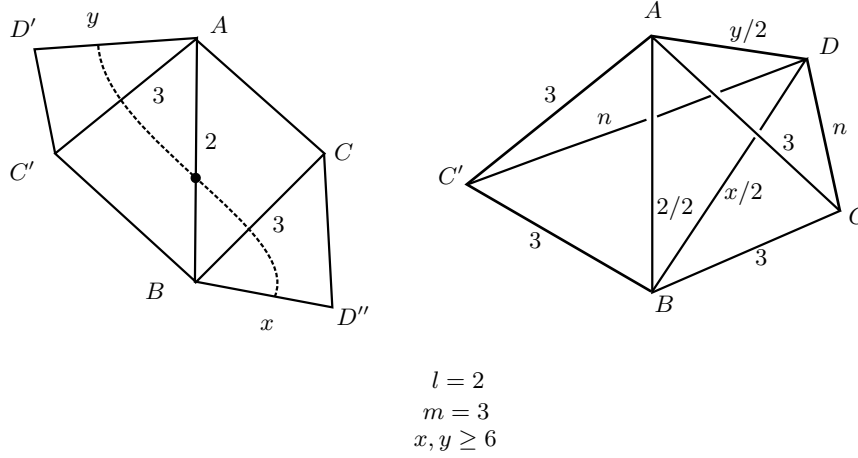
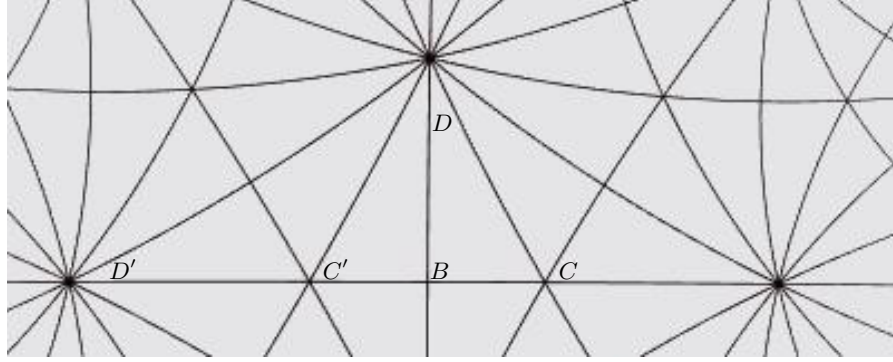


FIGURE 37. The case of Figure 32(ii). The upper half of the figure is the view from the vertex A , when $x = 7$.

can intersect at most two sides of the l -gon centered at B , and in this case those sides will always be $D'C'$ and DC' . It is clear that this circle is disjoint from the line $B'C^*$ representing Π_1 , and hence that $\Pi_1 \cap BC'D = \emptyset$. Now referring to the lower right part of the figure, we observe that $\Pi_2 = A'BD$ (as planes) and that the part of Π_2 that is on the same side of BCD as A is also on the *opposite* side of $BC'D$ as A . Since Π_1 is disjoint both from $BC'D$ and BCD (the latter by the previous case of Section 4.2.1), and because Π_1 lies on the same side of these planes as A , we can conclude that $\Pi_1 \cap \Pi_2 = \emptyset$ in this case when $l \geq 5$.

So we now assume that $l = 3$ in this case. We are not able to use the argument of the previous paragraph because some of the intersections ruled out in the previous paragraph can occur in this case. We refer to Figure 39. The possible values for q , n and p in the figure are based on the fact that the tetrahedron has no finite vertices. In this figure, $\Pi_1 = AC'A''B'$ and $\Pi_2 = A'B''DB$ (as planes). We determine that these planes are disjoint by a similar argument to the one given at the end of the

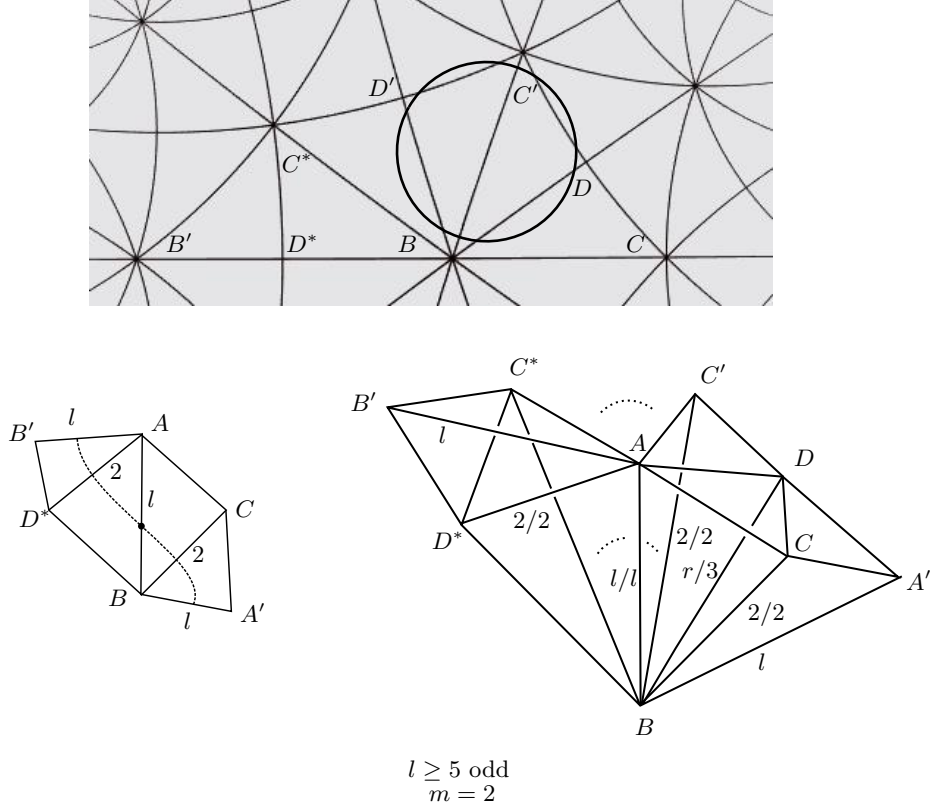


FIGURE 38. The case of Figure 32(i). The upper half of the figure depicts the view from the vertex A , in the case when A has type $(2, 4, 5)$.

paragraph on page 38 that dealt with case (iii) of Figure 32. This argument applies the techniques of Sections 4.1.1 and 4.1.2. In particular, if $n \geq 4$, then we use the geometry of the link of vertex C' to conclude that Π_1 is disjoint from the plane $BDC'D'$ (it lies to the same side of $BDC'D'$ as the vertex A) and the geometry of the link of vertex D to conclude that Π_2 is disjoint from the plane $ACDC'$ (it lies to the same side of $ACDC'$ as vertex B). Now by considering the plane ABD and the geometry of the vertex B , we have that the part of Π_2 that is on the C' side of ABD is always on the opposite side of $BDC'D'$ to Π_1 . Similarly, we have that the part of Π_1 on the D side of ABC' is always on the opposite side of $ACDC'$ to Π_2 . We conclude that $\Pi_1 \cap \Pi_2 = \emptyset$. When $n = 3$, the argument is similar, except that $ACDC' = ACB''DC'$ and $BDC'D' = BDC'A''D'$ (as planes) and we have that Π_1 and Π_2 form interior angles on the B side of $ACB''DC'$ of $3\pi/q \leq \pi/2$ and $\pi/r \leq \pi/6$, respectively (so that Π_1 and Π_2 cannot intersect on the side of this plane opposite to B), and interior angles on the A side of $BDC'A''D'$ of $\pi/q \leq \pi/6$ and $3\pi/r \leq \pi/2$, respectively (so that Π_1 and Π_2 cannot intersection on the side of this plane opposite to A). Again, we conclude that $\Pi_1 \cap \Pi_2 = \emptyset$. This completes case (i) of Figure 32, and concludes this subsection.

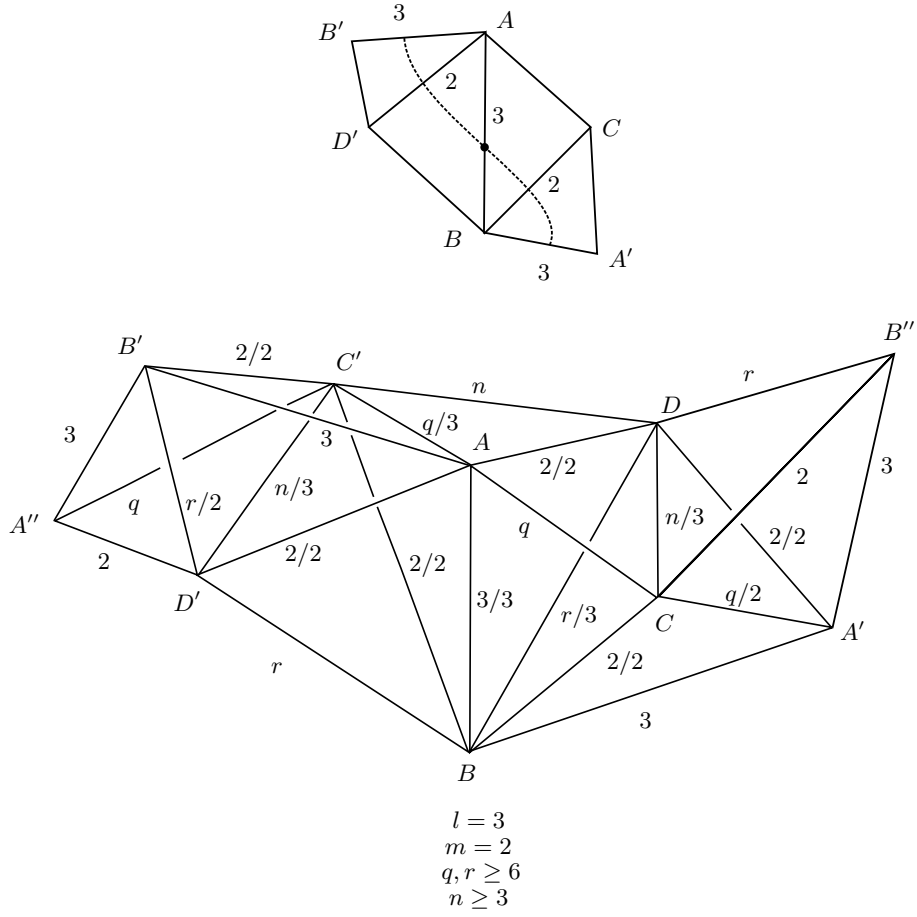
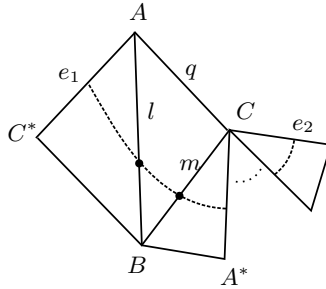
FIGURE 39. The case of Figure 32(i) when $l = 3$.

FIGURE 40. One case of Figure 21(a).

4.2.3. *21(a)*: See Figure 40, and recall the significance of the symbol “*” from Remark 3. We must first address the case when $e_2 = A^*C$. There are two possibilities that we must consider in determining whether or not Π_1 and Π_2 can intersect: either (1) Π_1 meets the plane through BC that is closest in inclination to the switch edge AB (it cannot meet more planes through BC , by our previous observations) and Π_2 meets

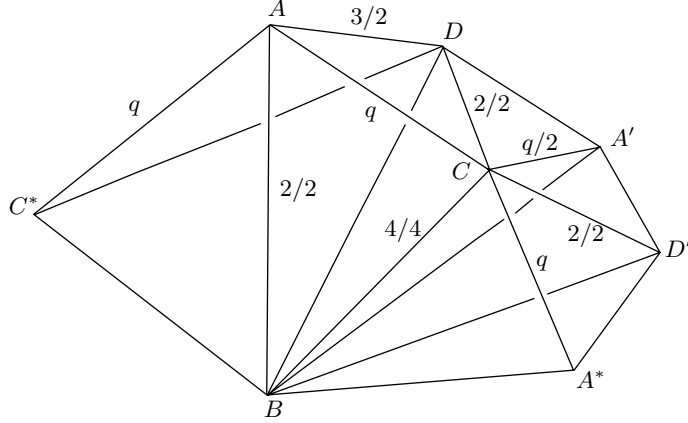


FIGURE 41. The case of Figure 40, when $l = 2$, $m = 4$ and $e_2 = A * C$.

at least the second closest plane through BC to the switch edge AB , or (2) Π_1 meets no planes passing through BC and Π_2 meets all of the planes passing through BC . We handle these two cases below:

- (1) In order for Π_1 to meet a plane passing through BC , our tetrahedron must take one of the forms of items (1)–(3) in the summary at the conclusion of the paper. This follows from the extensive analysis of Section 4.1 (in fact, the pairwise intersections of Π_1 , Π_F and the plane through BC inclined closest to the switch edge AB determine an immersed turnover in this case). We consider the case when $l = 3$, corresponding to item (3) in the summary. If $l = 3$, then $q = 2$, $m \geq 6$ and n (the order of the third edge associated to vertex C) is at least 3. It is then an easy analysis, using Figure 22, to see that there is no choice of n and m for which Π_2 can intersect either of the two closest planes through BC toward the edge AB . So $\Pi_1 \cap \Pi_2 = \emptyset$. Exactly the same analysis holds if our tetrahedron takes the form of item (1) of the summary at the conclusion of the paper (in this case we have $l = 2$, $m \geq 6$, $n = 2$ and $q \geq 3$, and so the order of edge A^*C is either 2 or q , and there is no choice for m and q such that Π_2 meets either of the two planes through BC inclined closest to the switch). If our tetrahedron has the form of item (2) from the summary, then $l = 2$, $m \geq 3$ and $q \geq 6$. If m is odd and at least 5, then the order of edge A^*C is 2 and we can use Figure 22 to conclude that Π_2 does not meet the two planes through BC inclined closest to the switch. If m is even and at least 6, then the order of A^*C is $q \geq 6$, and the conclusion of the previous sentence also holds. If $m = 4$, then we refer to Figure 41. Only the relevant edges are labeled in this figure, in which $\Pi_1 = AC^*D$ and $\Pi_2 = A^*D'A'C$. Because $q \geq 6$, we have that Π_1 and Π_2 form interior angles on the side of $ACA'D$ opposite to vertex B of $\pi/3$ and $(q - 2)\pi/q \geq 2\pi/3$, respectively (these are interior angles with respect to the edge CD). Therefore, Π_1 and Π_2 do not intersect on the side of this plane opposite to B . But, as we have observed,

$\Pi_1 \cap A'BC = \emptyset$. Since the part of Π_2 that is on the opposite side of $A'BC$ to Π_1 is always on the B side of $ACA'D$, we have $\Pi_1 \cap \Pi_2 = \emptyset$. The case when $m = 3$ is exactly the same. These are all the possibilities for when the tetrahedron has one of the types (1)–(3) in the summary. So $\Pi_1 \cap \Pi_2 = \emptyset$ for this case.

- (2) If the order of edge BC is greater than 4, then it is not possible to choose integers for the type of vertex C so that Π_2 crosses all the planes through BC . This follows by using the information of Figure 22, as in the arguments that accompany Figure 24 in Section 4.2.1. The same statement is true (with the same argument) if the order of BC is 3 and the vertex C has no incident order 2 edge. So the order of edge BC is either 3 and C has the type $(2, 3, x \geq 6)$ or the order of edge BC is 2. Suppose that the edge BC has order 3. Then we can use the same argument as the one given at the end of the previous paragraph. Namely, it is readily shown that Π_1 and Π_2 meet the plane containing the face ACD at interior angles that sum to at least π on the opposite side of ACD of the vertex B , and since they do not meet on the B side of this plane, they must be disjoint. The same argument also works when the order of BC is 2. So $\Pi_1 \cap \Pi_2 = \emptyset$ in this case.

So we can now assume $e_2 \neq A^*C$. We observe that removing the sides AC^* and BC^* from the diagram leaves a picture that is equivalent to the previous case of Subsection 4.2.1. We therefore know that Π_2 misses every plane through the switch edge AB . It follows, using Figure 22, that l must be either 2 or 3, in order for Π_1 to cross every plane through this switch edge. Moreover, we must have, as in previous cases, that the type of vertices A and C must include an order 2 point. Suppose $l = 2$. This implies that neither m nor q is 2. If, in addition, neither m nor q is 3, then it is straightforward using the information in Figure 22 to show that Π_2 cannot meet the plane through A^*C inclined closest to Π_1 , and so prove that $\Pi_1 \cap \Pi_2 = \emptyset$ in this case. So either $m = 3$ and $q \geq 6$ or $q = 3$ and $m \geq 6$, and in both cases $n = 2$. In either case, it is a straightforward application of the techniques already employed—specifically, the techniques involving developing tetrahedra from Sections 4.1.1 and 4.1.2—to show that Π_1 and Π_2 do not intersect.

Now suppose $l = 3$. Because Π_1 must cross every plane through the switch edge AB , it is easily shown using Figure 22 that the order of edge e_1 is at least 6 and $q = 2$. This implies that, if $m = 3$, then the order of the edge A^*C is also at least 6, in which case it is not possible for either Π_1 or Π_2 to meet the plane through A^*C that is inclined closest to the switch edge AB . So we must have $m \geq 6$. But now Π_1 will not meet the plane through BC that is second-closest inclined toward edge AB , and if $m \geq 7$, then it is readily seen (using the information in Figure 22) that Π_2 cannot intersect this second closest inclined plane, either. So we are left with $m = 6$. However, this case is easily handled using the techniques of the previous subsections.

4.2.4. *21(b)*: See Figure 42. Using our previous results, we conclude that it is not possible for Π_2 to meet any of the planes through the edge AC^* , and nor is it possible

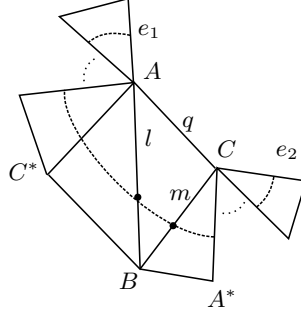


FIGURE 42. One case of Figure 21(b).

for Π_1 to meet any of the planes through the edge BC . Consequently, the intersection of Π_1 and Π_2 can only occur if Π_1 crosses every plane through AC^* and Π_2 crosses every plane through BC . The subsequent possibilities and arguments to rule them out are all straightforward to carry out, using the techniques we have employed to this point. This completes the proof. 1.2

Summary. We provide a summary of the classification of immersed turnovers in the orbifold \mathcal{O}_T associated to the generalized tetrahedron $T[l, m, q; n, p, r]$. These are listed in the order in which they appear in the proof, but isometric cases are indicated (the 24 isometric cases are determined by applying an element of the symmetric group S_4 : any element of the symmetric group S_3 may be applied to both the first and second triples of $T[l, m, q; n, p, r]$, and any pair from one triple may be swapped with the corresponding pair of the other triple). We also include a conjectural list of all the immersed turnovers in hyperbolic tetrahedral orbifolds. All of these can be confirmed using the techniques of this paper, and while the author believes this list to be exhaustive, the necessary computations to determine the complete classification are somewhat extensive.

- (1) $T[2, m, q; 2, p, 3]$. \mathcal{O}_T contains an immersed (q, m, p) turnover, where $q \geq 3, m \geq 6$ and $p \geq 6$.
- (2) $T[2, m, q; 2, 3, r]$ (isometric to item (1)). \mathcal{O}_T contains an immersed (q, m, r) turnover, where $q \geq 6, m \geq 3$ and $r \geq 6$.
- (3) $T[3, m, 2; n, p, 2]$ (isometric to item (1)). \mathcal{O}_T contains an immersed (m, n, p) turnover, where $m \geq 6, n \geq 3$ and $p \geq 6$.

Conjectural list of all immersed turnovers in hyperbolic tetrahedral orbifolds:

- (4) $T[2, m, q; 2, p, 3]$. \mathcal{O}_T contains an immersed (q, m, p) turnover for any of the following values:
 - (a) $q = 2, m = 4$ and $p \geq 5$. In this case, \mathcal{O}_T also contains
 - (i) a $(2, p, p)$ turnover,
 - (ii) a $(4, 4, 5)$ turnover if $p = 5$, and
 - (iii) a $(p/2, p, p)$ turnover if p is even.

- (b) $q = 2$, $p = 4$ and $m \geq 5$ (isometric to item (4), with the same set of additional non-maximal turnovers).
- (c) $q = 2$, $m \geq 5$ and $p \geq 5$. In this case, \mathcal{O}_T also contains
 - (i) a $(m, m, p/2)$ turnover if p is even, or
 - (ii) a $(m/2, p, p)$ turnover if m is even.
- (d) q , m and p are all greater than 2, and at least one is greater than 3. In this case, if two of the values are 3, then \mathcal{O}_T also contains a (x, x, x) turnover, where x is the integer that is greater than 3.
- (5) $T[3, 2, 2; 2, p, 3]$. \mathcal{O}_T contains an immersed $(2, p, p)$ turnover, where $p \geq 5$.
- (6) $T[3, m, 2; 2, p, 3]$. \mathcal{O}_T contains an immersed (m, p, p) turnover, where $m \geq 3$ and $p \geq 4$.
- (7) $T[3, m, 3; 2, 3, 2]$. \mathcal{O}_T contains an immersed $(3, m, m)$ turnover, where $m \geq 4$.
- (8) $T[4, 3, q; 2, 2, 2]$. \mathcal{O}_T contains an immersed $(q, q, 3)$ turnover, where $q \geq 4$.
- (9) $T[2, 2, 4; n, 3, r]$. \mathcal{O}_T contains an immersed turnover of type $(2, 4, r \geq 5)$ (as well as the additional non-maximal turnovers listed in item (4)) if $n = 2$, an immersed turnover of type $(4, 4, r \geq 3)$ if $n = 3$, and immersed turnovers of types $(3, 3, 5)$, $(3, 5, 5)$ and $(5, 5, 5)$ if $n = 2$ and $r = 5$.
- (10) $T[2, 3, q; 2, 3, r]$. \mathcal{O}_T contains an immersed (q, r, r) turnover, where $q \geq 3$ and $r = 4$ or $r = 5$.
- (11) $T[2, 2, q; 3, 5, 2]$. \mathcal{O}_T contains an immersed $(q, q, 5)$ turnover, where $q \geq 3$.
- (12) $T[2, 2, 5; 2, 3, 5]$. \mathcal{O}_T contains an immersed $(3, 5, 5)$ turnover.
- (13) $T[2, 2, 3; 3, p, 2]$. \mathcal{O}_T contains immersed turnovers of type $(3, p, p)$ and (p, p, p) , where $p = 5$ or $p = 6$ (also, $(2, p, p)$ by item (5) and $(3, 3, 5)$, when $p = 5$, by item (11)).
- (14) $T[2, 2, 3; 2, p, 3]$. \mathcal{O}_T contains immersed turnovers of type $(2, p, p)$, $(3, 3, p)$ and (p, p, p) if $p = 5$, and an immersed turnover of type $(3, p, p)$ if $p = 6$.

REFERENCES

- [1] Colin Adams and Eric Schoenfeld, *Totally geodesic Seifert surfaces in hyperbolic knot and link complements. I*, Geom. Dedicata **116** (2005), 237–247. MR 2195448
- [2] E. M. Andreev, *Convex polyhedra in Lobachevskii spaces*, Mat. Sb. (N.S.) **81** (**123**) (1970), 445–478. MR 0259734
- [3] ———, *Convex polyhedra of finite volume in Lobachevskii space*, Mat. Sb. (N.S.) **83** (**125**) (1970), 256–260. MR 0273510
- [4] Michel Boileau, Sylvain Maillot, and Joan Porti, *Three-dimensional orbifolds and their geometric structures*, Panoramas et Synthèses [Panoramas and Syntheses], vol. 15, Société Mathématique de France, Paris, 2003. MR 2060653
- [5] Daryl Cooper, Craig D. Hodgson, and Steven P. Kerckhoff, *Three-dimensional orbifolds and cone-manifolds*, MSJ Memoirs, vol. 5, Mathematical Society of Japan, Tokyo, 2000, With a postface by Sadayoshi Kojima. MR 1778789
- [6] William D. Dunbar, *Hierarchies for 3-orbifolds*, Topology Appl. **29** (1988), no. 3, 267–283. MR 953958
- [7] Craig D. Hodgson, *Deduction of Andreev's theorem from Rivin's characterization of convex hyperbolic polyhedra*, Topology '90 (Columbus, OH, 1990), Ohio State Univ. Math. Res. Inst. Publ., vol. 1, de Gruyter, Berlin, 1992, pp. 185–193. MR 1184410
- [8] C. Maclachlan, *Triangle subgroups of hyperbolic tetrahedral groups*, Pacific J. Math. **176** (1996), no. 1, 195–203. MR 1433988 (98d:20056)
- [9] Bernard Maskit, *Kleinian groups*, Grundlehren der Mathematischen Wissenschaften [Fundamental Principles of Mathematical Sciences], vol. 287, Springer-Verlag, Berlin, 1988. MR 959135

- [10] John W. Morgan, *On Thurston's uniformization theorem for three-dimensional manifolds*, The Smith conjecture (New York, 1979), Pure Appl. Math., vol. 112, Academic Press, Orlando, FL, 1984, pp. 37–125. MR 758464
- [11] Shawn Rafalski, *Immersed turnovers in hyperbolic 3-orbifolds*, Groups Geom. Dyn. **4** (2010), no. 2, 333–376. MR 2595095
- [12] John G. Ratcliffe, *Foundations of hyperbolic manifolds*, Graduate Texts in Mathematics, vol. 149, Springer-Verlag, New York, 1994. MR 1299730
- [13] Roland K. W. Roeder, John H. Hubbard, and William D. Dunbar, *Andreev's theorem on hyperbolic polyhedra*, Ann. Inst. Fourier (Grenoble) **57** (2007), no. 3, 825–882. MR 2336832
- [14] David Singerman, *Finitely maximal Fuchsian groups*, J. London Math. Soc. (2) **6** (1972), 29–38. MR MR0322165 (48 #529)
- [15] W. P. Thurston, *The geometry and topology of 3-manifolds*, Lecture notes from Princeton University, 1978–80.
- [16] William P. Thurston, *Three-dimensional manifolds, Kleinian groups and hyperbolic geometry*, Bull. Amer. Math. Soc. (N.S.) **6** (1982), no. 3, 357–381. MR 648524
- [17] ———, *Three-dimensional geometry and topology. Vol. 1*, Princeton Mathematical Series, vol. 35, Princeton University Press, Princeton, NJ, 1997, Edited by Silvio Levy. MR 1435975 (97m:57016)
- [18] Akira Ushijima, *A volume formula for generalised hyperbolic tetrahedra*, Non-Euclidean geometries, Math. Appl. (N. Y.), vol. 581, Springer, New York, 2006, pp. 249–265. MR 2191251
- [19] J. Weeks, *Kaleidotile*, <http://www.geometrygames.org/KaleidoTile/>.

DEPARTMENT OF MATHEMATICS AND COMPUTER SCIENCE, FAIRFIELD UNIVERSITY, FAIRFIELD, CT 06824, USA
E-mail address: `srafalski@fairfield.edu`